A WATER AND GREENHOUSE GAS INVENTORY FOR HYGROSCOPIC AND CONVENTIONAL EVAPORATIVE BUILDING-SCALE COOLING SYSTEMS

BY

JENNIFER CATHRYN NUGENT

THESIS

Submitted in partial fulfillment of the requirements
for the degree of Master of Science in Civil Engineering
in the Graduate College of the
University of Illinois at Urbana-Champaign, 2020

Urbana, Illinois

Adviser:

Associate Professor Ashlynn S. Stillwell

ABSTRACT

Freshwater scarcity is a major threat to the resilience of our society, and the challenges are only being exacerbated by the worsening impacts of climate change. The U.S. Department of Defense's Environmental Security Technology Certification Program demonstrated a novel heating, ventilation, and air conditioning (HVAC) cooling tower technology with the goal of reducing water usage. In this study, direct and indirect water usage and greenhouse gas emissions were quantified to analyze the tradeoffs associated with transitioning from a conventional wet-cooling HVAC tower to the novel hygroscopic system. Greenhouse gas emissions (GHG) were quantified for direct electricity consumption and the energy associated with water and wastewater conveyance and treatment using power plant and cooling system data, municipal water treatment data for California, and fuel-type emissions factors. Water usage was estimated using power plant data and cooling water factors from literature and the U.S. Energy Information Administration. It was found that the impact of increased electricity is greater than the indirect energy savings from the decrease in water usage, resulting in a net increase in GHG emissions. The indirect water consumption associated with cooling water for electricity generation is comparatively low when compared to the volume of direct water usage that is reduced by switching from conventional wet cooling to the hygroscopic system. The hygroscopic cooling technology shows promising water savings ability that will be more feasible in regions with extreme water scarcity, high water sourcing and treatment energy intensity, and/or when the electricity is sourced from low carbon-sources.

ACKNOWLEDGMENTS

Thank you to Ashlynn Stillwell for providing me with this opportunity to learn and grow as a researcher, and for always being supportive, understanding, and full of helpful advice. Thank you to the Stillwell Research Group for being a supportive group to bounce ideas off of or to share a commiseratory laugh with. A special thanks to Lauren Excell for her help with figure-making and acquiring and estimating water and wastewater utility data.

Thank you to the U.S. Army Construction Engineering Research Laboratory (CERL) and the Environmental Security Technology Certification Program (ESTCP) for giving me the opportunity to work on the Hygroscopic Cooling Tower project. Special thanks to Scott Lux with CERL and Dr. Christopher Martin with the Energy and Environmental Research Center (EERC).

Thank you to all the dogs — Newt, Goose, Obi, and Murph — for keeping me company through nights of coding, thesis writing, and a global pandemic, and for taking up all the space on my bed to prevent me from procrastinating. Honorary mention to Rigby and Penny.

Thank you to Maria and Steph for taking the time to proofread this thesis for me.

This work was financially supported by the US Army Construction Engineering Research Laboratory and the Department of Civil and Environmental Engineering at the University of Illinois at Urbana-Champaign.

TABLE OF CONTENTS

LIST OF ABBREVIATIONS

CCS	Carbon capture and storage
CERL	U.S. Army Construction Engineering Research Laboratory
CSP	Concentrated solar power
CWA	Clean Water Act
DCMB	DoD Center Monterey Bay
DoD	Department of Defense
EERC	Energy and Environmental Research Center
EIA	Energy Information Administration
EPA	Environmental Protection Agency
ESTCP	Environmental Security Technology Certification Program
GHG	Greenhouse gas
GIS	Geographic information system
HVAC	Heating, ventilation, and air conditioning
HX	Heat exchanger
MCWD	Marina Coast Water District
NOAA	National Oceanic and Atmospheric Administration
NPDES	National Pollution Discharge Elimination System
USGS	United States Geological Survey

LIST OF SYMBOLS

Bgal	Billion gallons
$CO_{2,eqv}$	Carbon dioxide equivalents
GJ	Gigajoule
km	Kilometers
km^3	Cubic kilometers
kW	Kilowatt
kWh	Kilowatt-hour
m^3/s	Cubic meters per second
MMBtu	Million British thermal units
MW	Megawatt
MWh	Megawatt-hour
MGal	Million gallons
MGD	Million gallons per day
RT	Refrigeration ton
TJ	Terajoule

CHAPTER 1

INTRODUCTION

Water scarcity is becoming an increasingly widespread problem as the effects of climate change and anthropological overuse and mismanagement progress [1]. Groundwater aquifers are rapidly depleting. Mountaintop glaciers that once supplied water are disappearing, and droughts are getting longer, harsher, and more frequent [2]. Freshwater is a commodity that has already been hard to come by in many regions of the world and this insecurity is worsening [3, 4]. From the 1990s to the 2000s, global water scarcity rose from affecting 14% of the global population to 58% [5].

The Department of Defense's (DoD) Environmental Security Technology Certification Program (ESTCP) is responsible for studying innovative environmental technologies as they move to field or production use. The ESTCP demonstrated a hygroscopic cooling system that was intended to reduce the heating, ventilation, and air conditioning (HVAC) water intensity of facilities that are currently using conventional evaporative cooling technology [6].

This analysis poses two research questions related to the hygroscopic cooling tower demonstration:

1. What are the greenhouse gas (GHG) implications of switching from a conventional wet cooling system to a hygroscopic system?

2. How does direct water savings at a building scale from the hygroscopic cooling system compare to indirect water usage at the power generation scale?

The answer to these questions will help determine the feasibility and benefit of the technology's application in practice and its contribution to reducing GHG emissions and increasing and water availability.

CHAPTER 2

BACKGROUND

Reducing the water consumed by cooling systems increases the resilience of Department of Defense (DoD) sites, especially in water-scarce regions. Cooling towers are common across DoD bases for building HVAC systems, data center cooling requirements, and for power generation; therefore, there is a notable opportunity for large water savings. Building cooling towers are a common piece of technology found not only on military bases but at office buildings, data centers, schools, and hospitals.

The DoD's Environmental Security Technology Certification Program (ESTCP) has demonstrated a novel hygroscopic cooling technology in two locations in California — Fort Irwin and the DoD Center in Monterey Bay (DCMB). Fort Irwin is located in southern California near the Mojave Desert, and the DCMB is located outside Monterey in the coastal city of Seaside. The hygroscopic cooling tower reduces the amount of makeup water required compared to conventional wet-cooling and eliminates wastewater generation, known as blowdown, by the HVAC system. Consequently, the hygroscopic system increases the amount of electricity required for operation compared to the traditional wet-cooling tower. The main performance objective of the ESTCP demonstration project is the evaluation of direct water savings. The other performance objectives include the quantification of electrical-to-thermal energy ratio, cooling tower performance, maintenance costs and efforts, economics, and an analysis of greenhouse gas emissions associated with direct and indirect electricity use for the cooling towers [6].

The changes in GHG emissions associated with the transition from a wet-cooling tower to a hygroscopic cooling tower were quantified by estimating the electricity required for HVAC tower operation, drinking water sourcing and treatment, and wastewater treatment. This information was used to compare the relationship of water savings and GHG emissions

between the building-scale cooling tower types.

The direct water usage and greenhouse gas performance objectives do not account for the water consumption and withdrawal that is required for cooling in most power generation stations. The impact of water consumption and withdrawal for cooling cannot be normalized by CO_2 equivalents the same way the drinking water was for the GHG analysis, because the cooling water for electricity generation applications is typically not treated.

2.1 Building-Scale Cooling Towers

There are two conventional types of building-scale cooling towers — dry-cooling and wet-cooling. There is also a third type, hybrid cooling towers, which combine dry- and wet-cooling systems into in parallel or series unit operations.

Dry cooling uses fans to cool the process working fluid. These systems have a cooling capacity that is limited by the ambient air temperature (dry-bulb temperature). Dry-cooled systems require less maintenance than wet-cooled systems, but in return they consume more electricity. California limits new dry cooling towers to a cooling capacity of 300 refrigeration tons due to the increased life-cycle cost of dry-cooled systems as a result of their high electricity consumption [7].

Wet-cooling towers are more efficient than their dry-cooled counterparts. Wet-cooling uses water for cooling, hence the name, and since water has a higher heat capacity than air, it absorbs heat more efficiently from the building-space that requires cooling. The water added to the cooling tower is known as makeup water. The heat from the building is absorbed by the cooling water and is rejected into the atmosphere. This evaporation rejects heat such that the cooling water cycles back through the cooling tower to absorb more heat. Although this process is more energy efficient than the dry-cooling process, the act of rejecting the heat to the atmosphere requires large amounts of water consumption through evaporation. For this reason, wet-cooling towers are also known as evaporative cooling towers. Much like perspiration is used to cool the human body, the process of evaporation cools the building-space.

Salt and chemical concentrations in the cooling water increase as the water evaporates.

The build-up of these solids in the cooling tower can lead to scaling within the system, corrosion of equipment, and microbial growth. To prevent these negative build-up effects, water is flushed from the system, known as blowdown, through a drain in the cooling tower, typically to the sewers. This process results in more water withdrawal and consumption by the cooling tower. Makeup water with high concentrations of salts and other chemicals requires additional water to effectively prevent build-up.

An alternative to traditional wet- and dry-cooling towers is hybrid cooling towers. Hybrid cooling towers combine wet- and dry-cooling technologies into a single system. Hybrid cooling towers are typically effective in situations where dry cooling towers were previously used, but require large tonnage chillers. Hybrid cooling towers only reduce water requirements by a maximum of 20% compared to conventional wet cooling towers [6].

2.2 Hygroscopic Technology

The hygroscopic cooling tower technology varies the sensible, or dry, and wet cooling by using a working fluid of calcium chloride ($CaCl_2$) [6]. The hygroscopic desiccant works by preventing evaporation of the cooling water — similar to silica gel packets that prevent moisture build up in consumer products.

The system adapts to ambient weather conditions, such as temperature and humidity. Unlike hybrid cooling systems that switch between dry and wet cooling systems, the hygroscopic system itself operates in a range of dry to wet operations [6]. This flexibility allows for more seamless operation and additional opportunity for water savings. By adapting to weather conditions, the system reduces the amount of makeup water required for cooling by taking advantage of sensible (dry cooling) heat when it is suitable for the ambient weather conditions [6]. Consequently, the hygroscopic system is able to approach the cooling efficiency of traditional wet-cooling towers and therefore could be used for large-tonnage chillers, unlike dry-cooling towers.

In addition to water savings accomplished by reducing evaporative cooling when it is efficient to do so based on ambient temperature and humidity, the hygroscopic cooling system also eliminates the blowdown stream [6]. All of the makeup water is evaporated, and the min-

eral build-up is removed from the hygroscopic system as a solid. By eliminating blowdown (the wastewater from flushing total dissolved solids), the system reduces water withdrawal and consumption and conserves the electricity required for treating the wastewater effluent. Because the mineral concentrations are removed as solids, the system can tolerate poorer makeup water quality without having to increase the amount of water required for flushing like a traditional wet-cooling tower [6]. Since the working fluid is tolerant of poor makeup water quality, the hygroscopic technology could be useful in remote locations or in future scenarios where water reuse systems are employed at DoD bases or in municipalities.

In addition, the $CaCl_2$ working fluid is nearly freeze-proof and it prevents microbial growth — issues that create a maintenance burden in traditional wet-cooling towers [6].

The hygroscopic technology was tested by integrating it into an existing wet-cooling tower. The hygroscopic system required an additional heat exchanger that connected the working fluid in the hygroscopic cooling tower to the fluid in the chiller that was responsible for the building's cooling load. The heat exchanger caused a higher temperature in the condenser and caused a drop in efficiency. The hygroscopic system requires the addition of this heat exchanger to integrate the hygroscopic system into the existing cooling tower [6].

The cooling tower data for both the conventional system and the hygroscopic system were processed to include and exclude the heat exchanger, to analyze how the heat exchanger affects the operation of the cooling tower. In future installments, the hygroscopic system could be constructed without this heat exchanger; however, this configuration would likely increase the capital cost required to entirely replace the existing wet-cooling tower.

The hygroscopic cooling tower was tested for three operational scenarios based on how aggressive water savings were being pursued. "Hygroscopic low" pursued the lowest water savings, and "hygroscopic high" pursued the highest water savings. The third operational scenario was "hygroscopic composite", and this mode picked the best operational scenario based on ambient weather conditions. The hygroscopic cooling tower was operated on each operational mode for part of the time and the data were later processed by Dr. Christopher Martin as if the tower had been operated for each scenario 100% of the operation time.

2.3 Demonstration Sites

The hygroscopic technology was tested at two locations in California to study the system's performance in different climates. The first system was implemented at Fort Irwin in the desert climate of southern California, just south of Death Valley National Park. The second system was integrated into an HVAC tower in the moderate coastal climate in Seaside along Monterey Bay.

The demonstration at Fort Irwin began in July 2018 and was installed on an existing tower that cools a 325-ton (1143 kW) chiller. Fort Irwin has an arid climate and pronounced day-to-night temperature fluctuations due to its location in San Bernardino County in the Mojave Desert. In Baker, CA about 35 miles (56 km) east of Fort Irwin, the minimum monthly average temperature is 47.6°F in December and the maximum monthly average is 93.7° F in July [8], based on data from 1981 to 2010.

The demonstration at the DCMB began in March 2019 and was implemented on an existing cooling tower that cools 190- and 120-ton (668 kW and 422 kW, respectively) staged chillers. The DCMB is located in Seaside, CA, outside Monterey, and has a coastal climate with limited diurnal temperature variation and ocean-moderated humidity. Temperatures in Monterey range from a minimum average of 50.8°F in December to a maximum average of 61.2° F in September [8].

During the time period of the demonstration, California was nearing the end of a drought that began in December 2011, with the most severe conditions spanning from 2014 to 2017 [9]. Drought conditions affect water usage across several industries, including agriculture and electric power generation. In the Central Valley of California from 2011 to 2014, the virtual water transfer of groundwater increased by 3.42 km^3 (903 billion gallons (Bgal)) to compensate for the decrease of precipitated and surface virtual water transfers by 0.94 km^3 (248 Bgal) and 1.96 km^3 (518 Bgal) respectively [10].

In terms of this study, the drought — in addition to environmental legislation and carbon prices — impacted the electricity generation resource mix of the region [11]. For California, this change in electricity generation sources presents itself as an increase in natural gas combustion to offset the decrease in hydroelectric power generation [12].

2.4 Hygroscopic Cooling Tower Demonstration

The "Hygroscopic Cooling Tower for Reduced HVAC Water Consumption" project was led by Dr. Christopher Martin of the Energy and Environmental Research Center (EERC) at the University of North Dakota. The other primary team responsible for this performing this demonstration was part of the U.S. Army Construction Engineering Research Laboratory (CERL) in Champaign, Illinois, led by Scott Lux. The demonstration's success was measured by the results of seven performance objectives: reduction in cooling tower water usage, limited increase in cooling tower energy usage, comparable cooling tower performance, reduction in system maintenance costs, no change in system maintenance efforts, 5-year payback on system costs, and reduction in net GHG emissions [6].

The first three performance objectives were related to the cooling tower water usage, energy usage, and performance. The next three objectives were related to maintenance cost, maintenance effort, and system economics. The final objective was related to an analysis of the GHG emissions associated with the energy and water consumption [6].

The success criteria for the cooling tower water usage and GHG emissions objectives were a 50% reduction for both makeup water and greenhouse gas emissions compared to the conventional cooling tower [6].

As part of a collaboration with the ESTCP and CERL, this analysis investigated the performance objective for the net change in GHG emissions associated with the transition from conventional evaporative cooling to the hygroscopic cooling system. The project boundary of this research includes:

- GHG emissions associated with direct electricity consumption by the cooling tower
- Emissions associated with the energy required for the sourcing, treatment, and distribution of drinking water (or possible alternative water source in the future) used by the HVAC cooling tower
- Emissions associated with the energy required for the treatment of wastewater (blowdown) produced by the conventional wet-cooling system

There is a gap in the analysis of greenhouse gas emissions and makeup water consumption that ignores the change in water withdrawn and consumed at the power generation scale. The secondary goal of this analysis was to fill this gap and provide a more complete understanding of the benefits and tradeoffs of switching from conventional wet cooling to hygroscopic cooling towers.

2.5 Water Withdrawal and Consumption

It is necessary to distinguish between the different types of water usage: withdrawal and consumption. Water withdrawal is the total quantity of water removed from a body of water and may or may not be returned to the same water source. Large water withdrawals can be seen in once-through cooling systems, where the water is removed — often from a surface water source — used in a condenser, and then returned to a surface water body at a higher temperature. Cooling water intake structures negatively affect aquatic organisms by trapping them against screens, or by harming them with heat or chemicals within the cooling system [13]. In terms of the hygroscopic cooling tower, the direct water withdrawal is the sum of the evaporated makeup water used and the blowdown wastewater produced by the HVAC cooling tower.

Water consumption is the fraction of withdrawal that is evaporated, transpired, or incorporated into products or crops [14]. For example, irrigation has high water consumption due to most of the water being evapotranspired by crops. The water footprint of production refers to this water consumption. With respect to this study, the water evaporated by the building-scale cooling towers is consumptive water use. For this analysis, final consumption is the total water consumed directly by the HVAC cooling tower and indirectly by the electricity generation systems supporting the grid.

In 2015, thermoelectric power generation made up 41% of total water U.S. withdrawals; of this 133 billion gallons of daily water withdrawal, once-through cooling systems accounted for 96% of the total power plant withdrawals [14]. Total consumptive water use by thermoelectric power plants made up only 3% of the total withdrawals [14].

There is currently no standard among the literature for estimating the water usage asso-

ciated with electricity generation. Typically, net electricity generation data for U.S. power plants are obtained from Form EIA-923 [15], such as in Marston et al. (2018) and Zohrabian and Sanders (2018) [16, 17].

Disagreement in the literature come with respect to which water withdrawal and consumption coefficients to use for estimating thermoelectric water usage. The United States Geological Survey (USGS) published a report on "Withdrawal and Consumption of Water by Thermoelectric Power Plants in the United States" with water usage coefficients in both 2010 and 2015 [18, 19], which were used to estimate water usage in Marston et al. (2018) [16]. In another analysis, Macknick et al. (2012) provides withdrawal and consumption factors aggregated from literature for electricity generation by fuel type, technology, and cooling system type [20]. Macknick et al. (2012) is also commonly cited in estimates of electricity generation withdrawal and consumption estimates, such as in Zohrabian and Sanders (2018)[17].

Further disagreement in the literature come with respect to the proper methodology for estimating water consumption associated with reservoirs and hydroelectric generation. Gross evaporation refers to the rate of total evaporation from the reservoir, while net evaporation is the change in evaporation with respect to the land-use before the reservoir was inundated. Although net evaporation is widely understood to be the preferred method of estimation, much of the literature still uses consumption coefficients based on gross evaporation. Macknick et al. (2012) cites factors based on the gross evaporation estimates of 4.7 m^3/GJ (1200 gal/GJ) [21] and 17 m^3/GJ (4500 gal/GJ) [22]. Grubert (2016) estimated the net evaporation for hydropower reservoirs to be 1.7 m^3/GJ (450 gal/GJ) and gross evaporation to be 11 m^3/GJ (2900 gal/GJ) [23]. By using consumption coefficients based on gross evaporation, hydroelectric water consumption is greatly overestimated.

2.6 Greenhouse Gas Emissions Quantification

Greenhouse gas emissions associated with electricity generation are emitted at multiple stages of the processes' life cycle (depending on the energy source), including raw material extraction and combustion. For non-combustible fuels, like solar, hydro, wind, and nuclear,

GHG emissions are associated with the mining of raw material, transportation, and the production of equipment. For fossil fuels (e.g., natural gas and coal), greenhouse gases are emitted during mining, fuel storage and transportation, and combustion.

In literature, often many of these life-cycle emissions are neglected, and GHG emissions are calculated only for the combustion of fuels [17]. GHG emissions associated with fuel combustion are typically calculated using net electricity generation data from Form EIA-923 and EPA emissions factors for the given fuel type [15, 24].

2.7 Energy Intensity of Water and Wastewater Treatment

The electricity consumption for sourcing, conveying, and treating water and wastewater is dependent on the source type, water quality, the distance of conveyance, and the treatment methods (which are dependent on end-use). Estimates of the average embedded energy for drinking water sourcing, treatment, and distribution in literature range from 1287 kWh/Mgal [25] to 1900 kWh/Mgal [26].

Southern California had the highest water energy intensity within the United States; transporting water from Northern California to Southern California required about 11,000 kWh/Mgal (2900 kWh/1000 m^3) and the total estimated energy intensity of water-wastewater cycles in Southern California was 13,000 MWh/Mgal (3400 kWh/1000 m^3) [27]. In particular, reverse osmosis for desalination required 13,200 – 26,500 kWh/Mgal (3,490 - 7,000 kWh/1000 m^3) [27].

CHAPTER 3

GREENHOUSE GAS INVENTORY

3.1 Introduction

As part of the analysis of the ESTCP hygroscopic cooling system demonstration, the conventional and hygroscopic system were compared based on both direct and indirect electricity usage and the greenhouse gas emissions associated with this electricity consumption.

The GHG emissions performance objective motivated the following research questions:

- What are the specific GHG implications of water conservation at the demonstration sites?
- Are there locations with unrecognized potential for GHG reductions through water conservation?
- How might future water source alternatives (e.g., inland desalination) impact GHG projections?

3.2 Methods

The project boundary for analyzing the GHG emissions associated with direct and indirect electricity usage was comprised of three main components: water treatment, electricity generation, and wastewater treatment. The project boundary is depicted in Figure 3.1.

"Direct emissions" refer to emissions associated with the electricity used directly by the HVAC cooling tower located at the DoD facilities. "Indirect emissions" are those associated with the energy required for sourcing, treating, and conveying water to the HVAC cooling

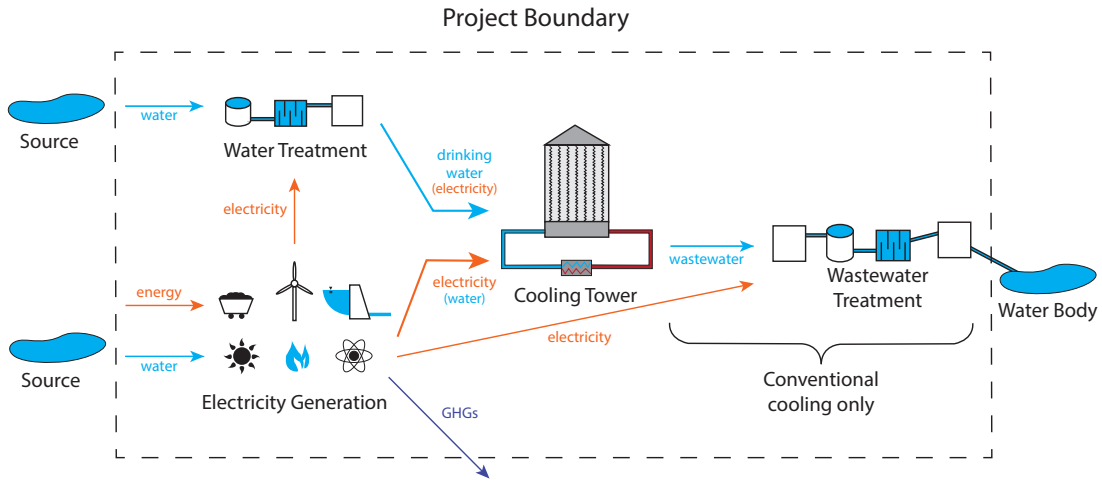

Figure 3.1: The project boundary includes the greenhouse gases associated with the direct and indirect water and energy usage required for operation of the cooling tower. Indirect water and energy usage results from electricity generation, and water and wastewater treatment.

tower, as well as the electricity required for treating the wastewater discharged from the cooling tower.

Greenhouse gas emissions factors (in lbs of $CO_{2,eqv}$/MWh) were developed based on Energy Information Administration (EIA) electricity generation data for California's electricity generation stations provided in Form EIA-923 [15]. Form EIA-923 provides fuel type information, total monthly fuel consumption, and total electric fuel consumption (in MMBtu). The Environmental Protection Agency (EPA) provides emission factors for CO_2 (carbon dioxide), CH_4 (methane), and N_2O (nitrous oxide) [24] for the combustion of a variety of fuels. CO_2 equivalents is defined as the summation of the emission factors for these three greenhouse gases. For the purpose of this analysis, CO_2 equivalents were used to compare the hygroscopic and the pre-existing evaporative cooling towers.

EPA emissions factors were assigned for the primary energy carriers and starter fuel sources used in energy production. Primary energy carriers include the following fuel types: natural gas, bituminous coal, and landfill gas. Wood and wood waste solids and agricultural by-products are often co-fired or used for a stand alone boiler. Other co-fired fuels include solid petroleum coke and tire-derived fuels. Starter fuels include kerosene, distillate fuel oil, jet fuel, propane gas, and other biomass gases. Starter fuels are combusted in small volumes

Table 3.1: Relevant EPA Emissions Factors from 2018 [24].

Fuel Type	**CO_2 Factor (kg/MMBtu)**	**CH_4 Factor (kg/MMBtu)**	**N_2O Factor (kg/MMBtu)**
Agricultural By-Products	118.17	32	4.2
Bituminous Coal	93.28	11	1.6
Distillate Fuel Oil No. 1	73.25	3.0	0.60
Distillate Fuel Oil No. 2	73.96	3.0	0.60
Distillate Fuel Oil No. 4	75.04	3.0	0.60
Jet Fuel	72.22	3.0	0.60
Kerosene	75.20	3.0	0.60
Landfill Gas	52.07	3.2	0.63
Natural Gas	53.06	1.0	0.10
Other Biomass Gas	52.07	3.2	0.63
Petroleum Coke (Solid)	102.41	3.0	0.60
Propane Gas	61.46	3.0	0.60
Residual Fuel Oil No. 5	72.93	3.0	0.60
Residual Fuel Oil No. 6	75.10	3.0	0.60
Tire-Derived Fuels	85.97	32	4.2
Wood and Wood Residuals	93.80	7.2	3.6

to provide start-up power in thermoelectric power plants, which rely mostly on the primary fuel for producing the electricity output. These factors are summarized in Table 3.1

Average emissions factors were used for distillate fuel oil and residual fuel oil. For distillate fuel oil, an average of the factors for distillate fuel oils No. 1, No. 2, and No. 4 was calculated and used. For residual fuel oil, an average of residual fuel oil No. 5 and No. 6 was applied.

Using the monthly electric fuel consumption from EIA-923 and the EPA emissions factors, monthly GHG emissions were estimated for electricity production. With California-specific GHG emissions factors for electricity generation and monthly electricity usage reported from the demonstration cooling towers, GHG emissions related to electricity usage were calculated.

Drinking water and wastewater treatment data were obtained to calculate monthly electricity consumption associated with the HVAC cooling systems' water usage. The water and wastewater treatment utilities for Seaside, California, were identified and contacted. Data were not available from the water and wastewater utilities that serve the Fort Irwin training center.

The Seaside wastewater utility was identified through the Seaside municipal water website

to be Monterey One Water. The Clerk to the Board of Directors provided monthly electricity consumption and treatment flow data for 2018 and 2019 (Figure 3.2). These data were validated by comparing to wastewater treatment data for major cities in California from the HydroShare database prepared by Chini and Stillwell [28]. The wastewater intensity data from 2019 were used to estimate the GHG emissions associated with wastewater produced by the conventional HVAC cooling tower at the DCMB and Fort Irwin.

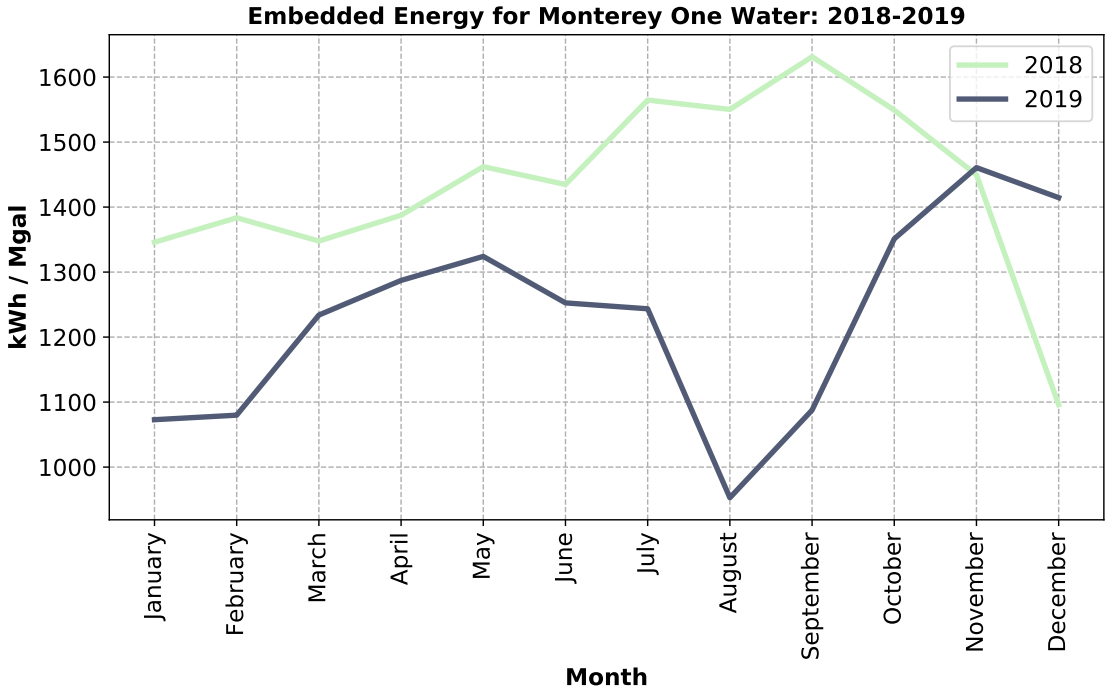

Figure 3.2: The embedded energy (kWh/Mgal) from Monterey One Water for 2018 and 2019.

Through 2008 GIS data for the City of Seaside, the Marina Coast Water District (MCWD) was identified as the drinking water treatment facility for the DCMB facility. Water treatment data were not received from the MCWD. Alternatively, values for electricity consumption for water treatment and treated water flows were estimated based on information published on the MCWD website. The MCWD withdraws approximately 3,200 acre-feet per year (2.8 million gallons per day) from groundwater sources [29]. The supply wells for the Ord Community, where the DCMB is located, obtain groundwater from the 180-foot and 400-foot aquifers of the Salinas Valley Groundwater Basin, and the water is treated by disinfection [29]. The unit electricity consumption for a 2.8 MGD treatment plant was

linearly interpolated from the data published by the Electric Power Research Institute [26], leading to an estimate of 1453 kWh/gal. Therefore, the MCWD drinking water treatment plant was estimated to use 4151 kWh/day to source and treat its water in the absence of recorded data.

Fort Irwin water and wastewater energy intensity data were not available. To provide an estimate for the wastewater treatment intensity for southern California, San Diego wastewater utility data from 2012 were used [28]. The San Diego water treatment plant had a monthly average of 632 kWh/Mgal in 2012; however, this value was a conservative estimate for drinking water embedded energy for the remote desert site of Fort Irwin when compared to the literature.

Instead, the interpolated water treatment energy intensity for Seaside (1453 kWh/Mgal) was used in water treatment calculations for Fort Irwin to provide a more realistic estimate for the high water sourcing and treatment energy intensity in southern California. Using these water and wastewater energy intensity factors and monthly water consumption and wastewater effluent values reported from the demonstration cooling towers, GHG emissions related to water usage by the HVAC cooling towers were calculated.

Figure 3.3 provides a simplified depiction of these methods.

The uncertainty for emissions associated with water and wastewater usage was calculated using water and wastewater treatment utility data from major cities across the United States [25]. The energy intensity for water and wastewater treatment utilities in California, and especially southern California, are some of the highest energy intensities in the country. To calculate uncertainty, a min-max method was used with the 50^{th} percentile data from Chini and Stilwell [25] plus and minus one standard deviation. The 25^{th} and 75^{th} percentile values for energy intensity values were not used as minimum and maximum values because the California water and wastewater treatment energy intensity is often greater than the 75^{th} percentile value.

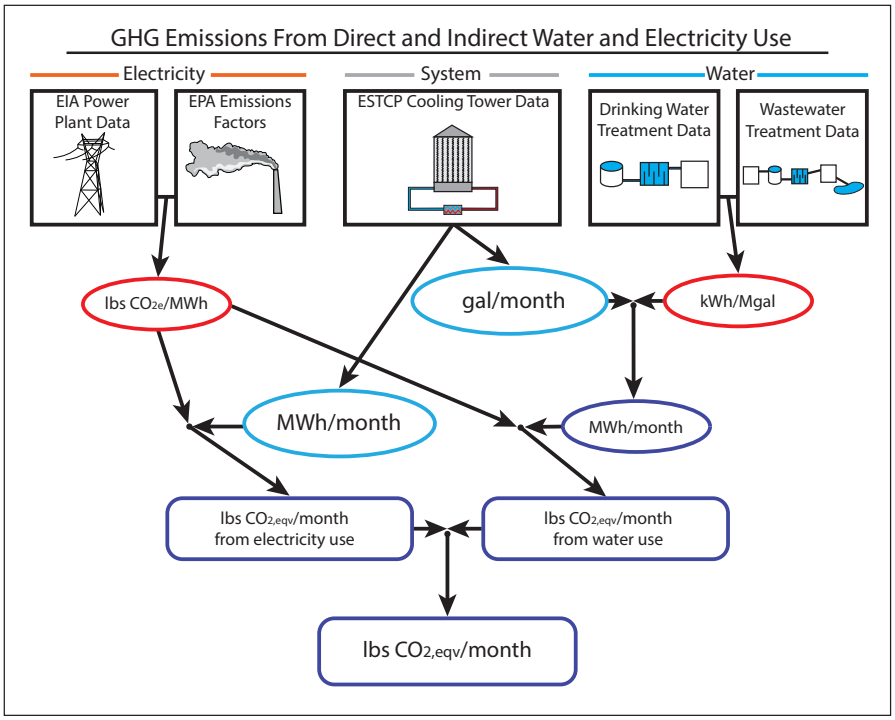

Figure 3.3: The process of estimating GHG emissions includes EIA electricity generation data, EPA emissions factors, water and electricity usage data from the cooling towers used in the demonstration, and water and wastewater treatment energy intensity data and estimation; the black rectangles represent these sources of data. The blue ovals represent direct water and energy data from the cooling tower, which have the greatest impact on associated GHG emissions and water usage. The red ovals are electricity and water factors. The purple oval and rectangles represent calculated values, and the purple rectangles signify results of the analysis.

3.3 Results

3.3.1 Greenhouse Gas Emission Factors for California

Emissions factors for electricity generation vary seasonally and annually and are dependent on the resource mix of primary fuels used for electricity generation. California experienced an extended drought from 2011 until 2019 [9]. During periods of drought, California switches some energy production from hydropower to natural gas [12]. In addition to this drought-related fuel shift, over the last decade coal plants have been phased out in California. Therefore, natural gas is the main source of GHG emissions in California's energy sector.

As California passed legislation to reduce GHG emissions [30] and as the drought conditions have improved, the monthly emissions factors for energy production have decreased over time. This trend can be seen in Figure 3.4, which shows the extensive annual variation in monthly $CO_{2,eqv}$ emissions factors from 2010-2018.

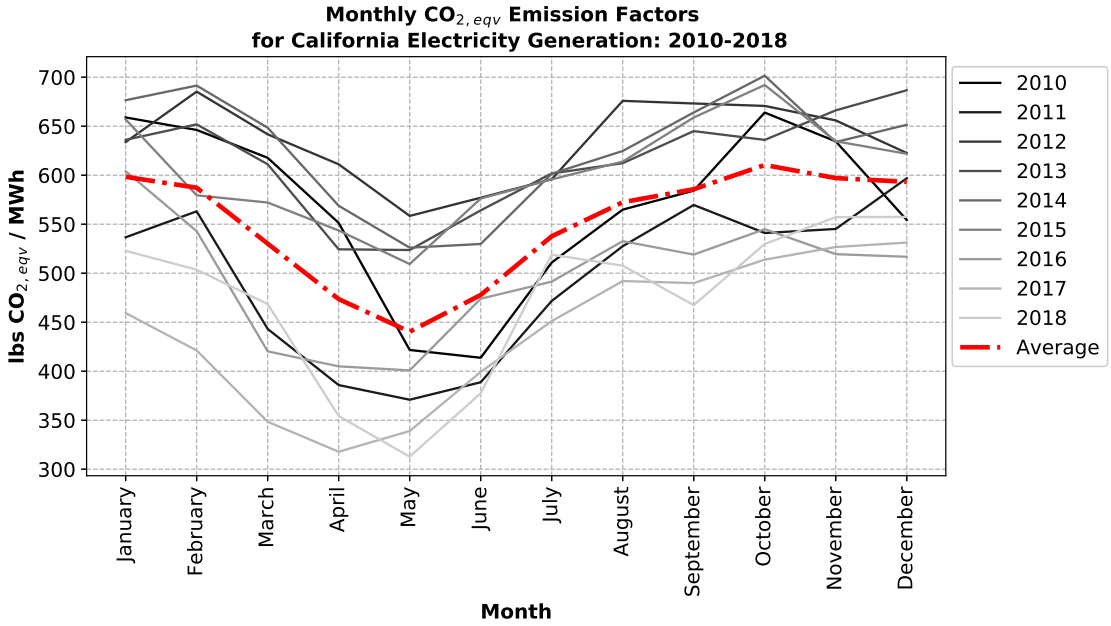

Figure 3.4: Monthly $CO_{2,eqv}$ emission factors for California from 2010 to 2018 vary monthly and annually. Each grey line represents a year from 2010-2018; 2010 is represented by the darkest grey line and 2018 is represented by the lightest grey line. The red line represents the average monthly factors for the nine-year span.

Shown in Figure 3.5, the greatest range in emission factors occurred from February to June, with standard deviations of 80.3 $CO_{2,eqv}$/MWh in June to 104.9 $CO_{2,eqv}$/MWh in March.

March and April (104.9 and 101.3 $CO_{2,eqv}$/MWh, respectively) had the highest standard deviations presumably due to the variation in snow melt coming from the mountains in the spring [31] and high winter precipitation due to the westerlies winds that bring moisture from the Pacific Ocean over California. Monthly emission factor averages were used to calculate the following estimates for GHG emissions.

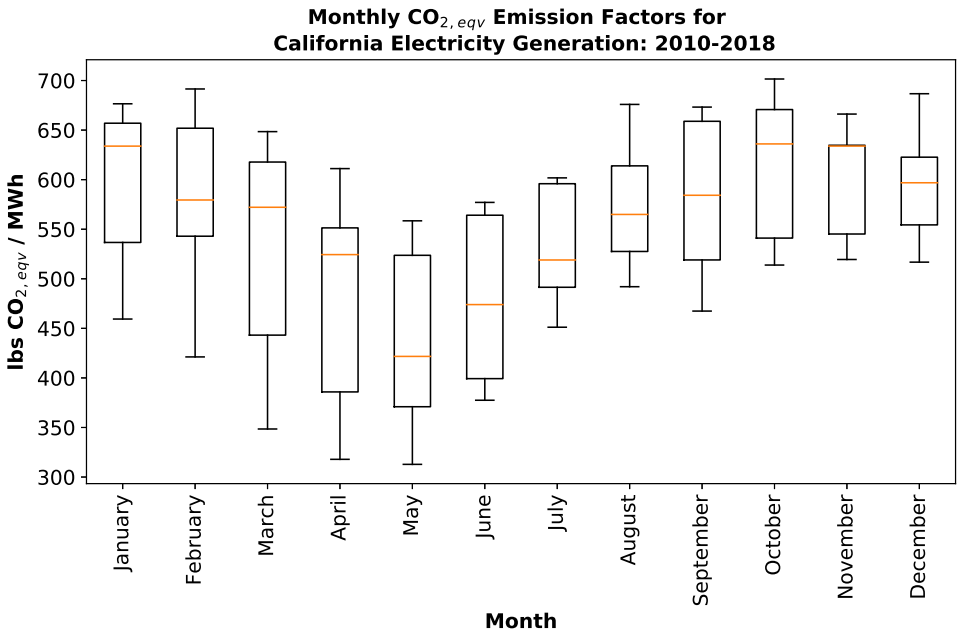

Figure 3.5: Monthly $CO_{2,eqv}$ emissions factors in California vary over the analysis time of 2010-2018

3.3.2 Total Greenhouse Gas Emissions from Direct Electricity and Water Use

The data from the HVAC cooling towers breaks down into 8 different test scenarios – with and without heat exchanger (HX), and then into conventional cooling, hygroscopic low, hygroscopic high, and hygroscopic composite. A heat exchanger was present in the hygroscopic system and not the conventional wet cooling tower and it operated between the working fluid in the hygroscopic cooling tower and the fluid in the chiller. The heat exchanger resulted in a performance penalty, so the data were processed for a scenario that included the heat exchanger and another that did not include it. Due to this performance penalty, the GHG gas emissions estimates were higher for the scenario where the heat exchanger was included.

The hygroscopic systems were operated at three different levels. "Hygroscopic low" was when the least aggressive water savings were pursued, and "hygroscopic high" was when the maximum water savings were pursued. "Hygroscopic composite" selected the best op-

erational scenario for the ambient weather conditions. "Conventional cooling" refers to the operation of the pre-existing wet-cooling HVAC tower that did not use the hygroscopic working fluid.

The majority of the total monthly GHG emissions were associated with direct electricity use. As a result of the increased operational electricity demand, associated GHG emissions increased when the system was switched from conventional wet-cooling to the hygroscopic tower. However, if the hygroscopic system were compared to a dry-cooling system, the hygroscopic system may have lower GHG emissions estimates.

Figures 3.6 and 3.7 provide the emissions estimate for the DCMB and Fort Irwin cooling towers, respectively, in terms of pounds of CO_2 equivalents per refrigeration ton (RT) of cooling capacity. GHG emissions for the DCMB cooling tower were highest for the "hygroscopic high" and "hygroscopic composite" scenarios, while emissions for the "hygroscopic low" were relatively similar to the conventional system.

Cooling tower operation at the DCMB was lower in July; the cause of this decrease in operation is unknown. A similar yet less extreme decrease in operation also occurred in May.

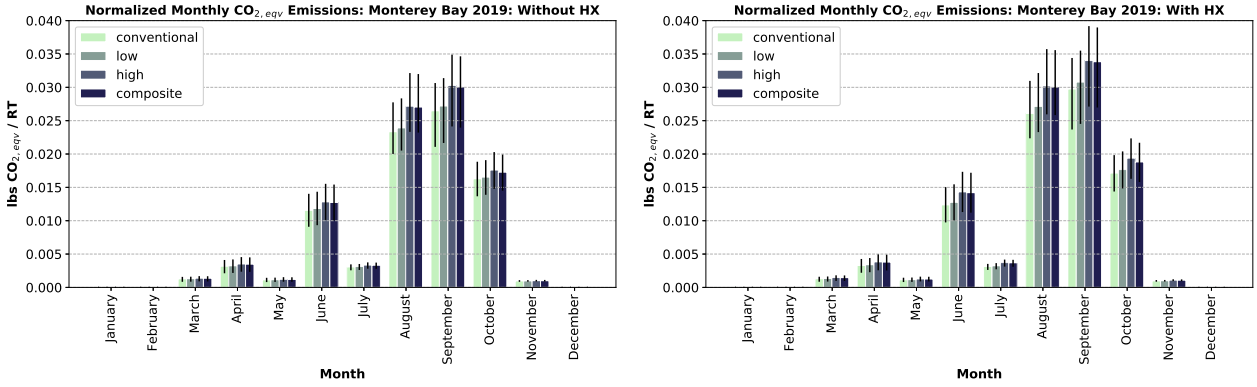

(a) Without Heat Exchanger

(b) With Heat Exchanger

Figure 3.6: The total monthly emissions (in $CO_{2,eqv}$) for the DoD Center Monterey Bay (DCMB) cooling tower in 2019 were normalized by refrigeration ton (RT) of the cooling tower capacity.

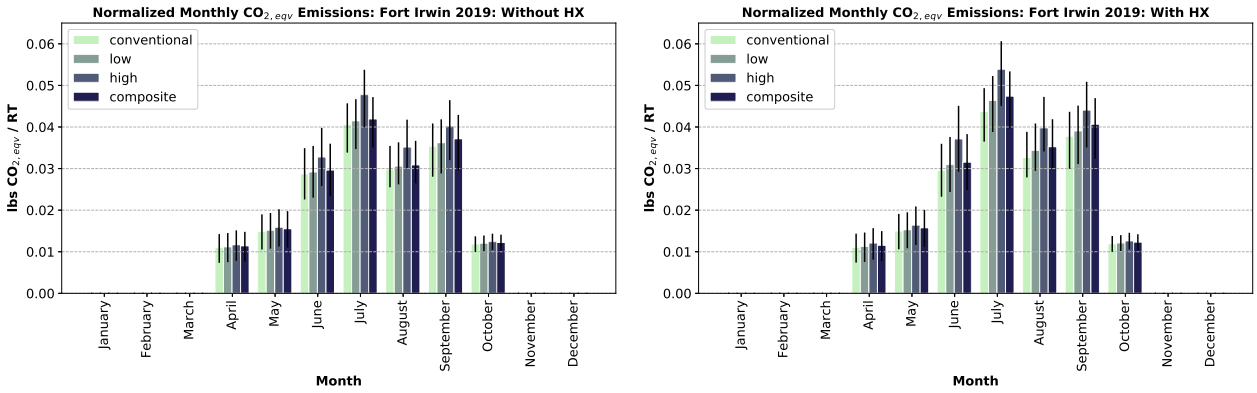

(a) Without Heat Exchanger

(b) With Heat Exchanger

Figure 3.7: The total monthly emissions (in $CO_{2,eqv}$) for the Fort Irwin cooling tower in 2019 were normalized by refrigeration ton (RT) of the cooling tower capacity.

For Fort Irwin, GHG emissions were highest for the "hygroscopic high" scenario; emissions associated with "hygroscopic low" and "hygroscopic composite" scenarios were more similar to the conventional system. This result suggests that the "hygroscopic composite" is more beneficial and effective in arid climates than it is in moderate, coastal climates.

Fort Irwin has higher temperature extremes than Monterey; consequently, the cooling requirements are greater, and the process requires more energy. Therefore, the GHG emissions associated with water savings were greater in Fort Irwin than in Monterey Bay. In addition to this difference, water acquisition is more energy intensive in southern California than it is in Monterey Bay. To further compare the difference in emissions in Monterey and Fort Irwin, the GHG emissions were normalized by the cooling capacity of the systems' chillers.

The data were normalized by refrigeration ton (RT). A ton of refrigeration is a North American unit of power used to define cooling and refrigeration capacity. The demonstration system was integrated into an existing cooling tower at the DCMB that employed 190-ton and 120-ton, staged chillers. The hygroscopic system at Fort Irwin was integrated into an existing unit with a 325-ton cooling capacity chiller.

The raw, non-normalized versions of the figures in this section are provided in Appendix A, which includes the total monthly quantities of GHG emissions for both demonstration sites, as well as the normalized and non-normalized figures of the same values for Fort Irwin's operation in 2018.

3.3.3 Greenhouse Gas Emission from Direct Electricity Use

Direct electricity consumption by the HVAC cooling towers was responsible for a majority of the GHG emissions associated with building cooling.

Monthly GHG emissions estimates associated with the electricity consumed directly by the cooling tower in Monterey Bay are shown in Figure 3.8. During months of relatively low electricity use, all four scenarios had similar GHG emissions. Conversely, when more electricity was consumed, the difference in emissions for each scenario was greater. "Hygroscopic high" and "hygroscopic composite" consistently resulted in higher GHG emissions as a result of the additional electricity needed to obtain the greater water savings. The "high" and "composite" hygroscopic operational modes used the greatest amount of electricity to achieve water savings at the DCMB.

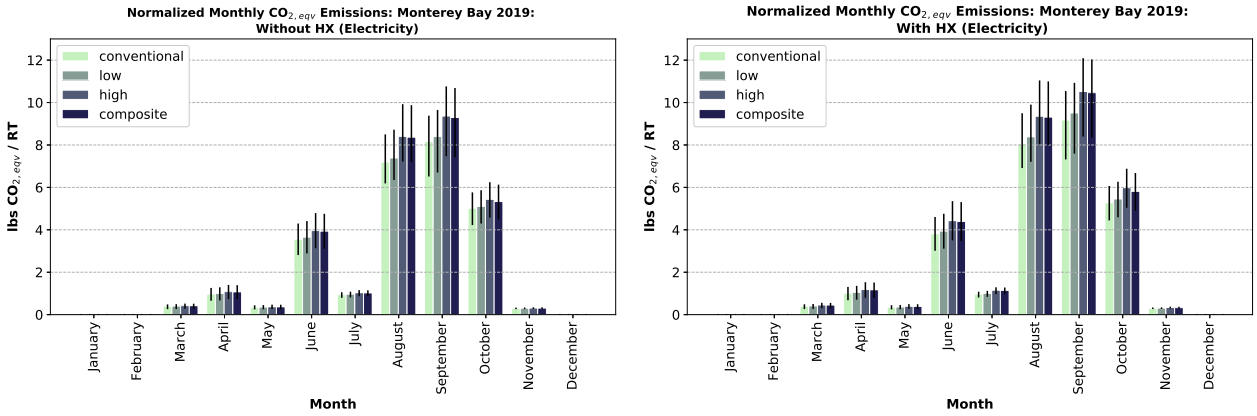

(a) Without Heat Exchanger (b) With Heat Exchanger

Figure 3.8: The monthly emissions (in $CO_{2,eqv}$) associated with direct electricity usage for the DoD Center Monterey Bay (DCMB) cooling tower in 2019 were normalized by refrigeration ton (RT) of the cooling tower capacity.

Monthly GHG emissions estimates associated with the electricity consumed directly by the cooling tower at Fort Irwin are shown in Figure 3.9. Like Monterey, all four scenarios had relatively similar GHG emissions during months with lower electricity usage. "Hygroscopic high" used the greatest amount of electricity to achieve the maximum water savings and was responsible for the highest emissions, as shown in the figures of total GHG emissions in the previous section.

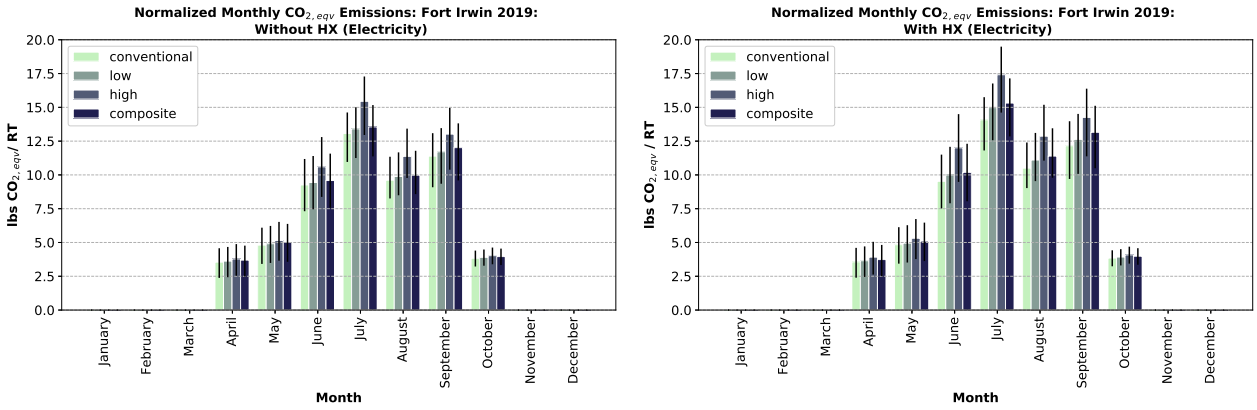

(a) Without Heat Exchanger

(b) With Heat Exchanger

Figure 3.9: The monthly emissions (in $CO_{2,eqv}$) associated with direct electricity usage for the Fort Irwin cooling tower in 2019 were normalized by refrigeration ton (RT) of the cooling tower capacity.

3.3.4 Greenhouse Gas Emissions Associated with Makeup Water Evaporation

The hygroscopic cooling tower was successful in its goal of reducing total makeup water usage. Total makeup water usage is the sum of evaporated makeup water and blowdown that is discharged to the sewer; the former will be analyzed in this section.

For the coastal climate at the DCMB, the hygroscopic "high" and "composite" scenarios were the most successful in reducing water consumption. The greenhouse gas savings for the "hygroscopic low" scenario were relatively low. Figure 3.10 shows the large amount of uncertainty that surrounds the GHG estimates for make-up water use.

Uncertainty surrounding the water treatment energy intensity is high not only due to the limited data available from municipalities local to the demonstration sites, but because the energy intensity fluctuates monthly and annually due to a number of factors. Uncertainty was propagated using utility data from the United States, which also explains the large range of uncertainty [25]. Although the uncertainty is high, the GHG emissions associated with makeup water treatment contributed minimally to total GHG emissions for the cooling tower, and therefore has a negligible effect on the total estimates for GHG emissions.

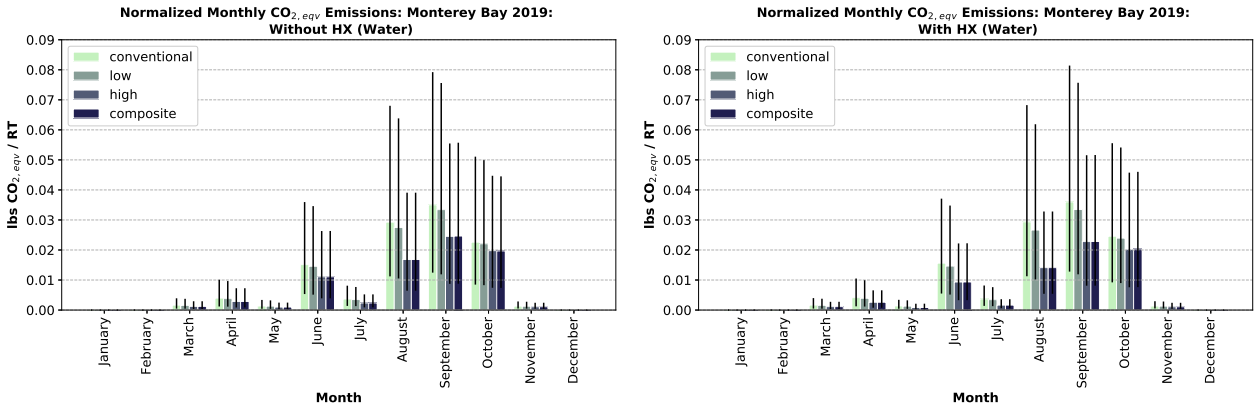

(a) Without Heat Exchanger (b) With Heat Exchanger

Figure 3.10: The monthly emissions (in $CO_{2,eqv}$) associated with direct water consumption by the DoD Center Monterey Bay (DCMB) cooling tower in 2019 were normalized by refrigeration ton (RT) of the cooling tower capacity.

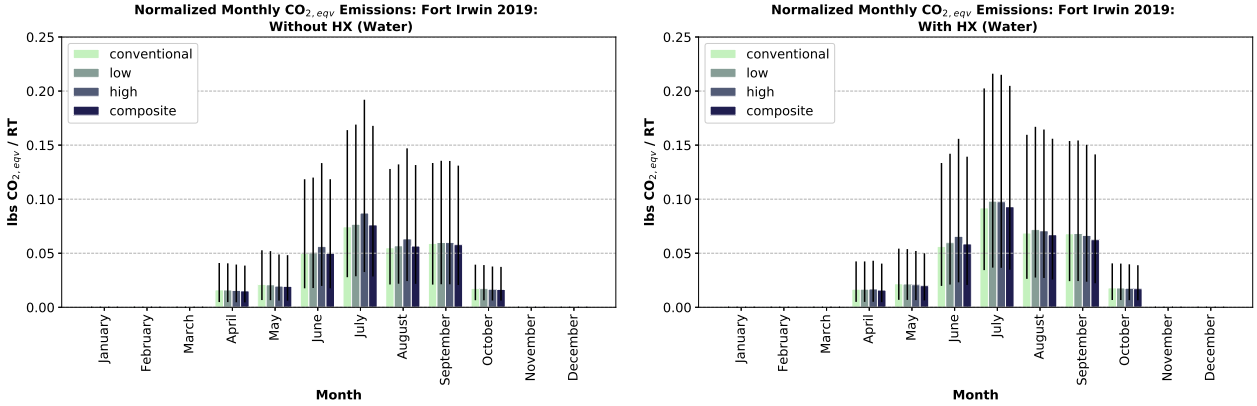

(a) Without Heat Exchanger (b) With Heat Exchanger

Figure 3.11: The monthly emissions (in $CO_{2,eqv}$) associated with direct water consumption by the Fort Irwin cooling tower in 2019 were normalized by refrigeration ton (RT) of the cooling tower capacity.

Figure 3.11 shows the emissions associated with the water evaporated by the Fort Irwin cooling tower. Although the hygroscopic system led to significant overall water savings at the Fort Irwin cooling tower, this reduction was mostly due to the elimination of blowdown. The "hygroscopic high" scenario had the highest makeup water consumption during multiple months. Consequently, there are no clear trends in the values shown in Figure 3.11; the emissions values in Figure 3.11b are relatively similar for all scenarios.

3.3.5 Greenhouse Gas Emissions from Wastewater Discharge

The hygroscopic system eliminates system blowdown; therefore, wastewater discharges only occurred for the conventional system. In the hygroscopic system, all the makeup water is evaporated, and mineral build-up is removed as a solid, rather than being flushed to the sewer via blowdown. By eliminating blowdown, the hygroscopic system significantly reduces water usage compared to the conventional wet-cooling tower.

GHG emissions associated with wastewater discharge are based on the energy intensity of wastewater treatment. While the elimination of blowdown reduces GHG emissions associated with the hygroscopic system, the reduction is on a much smaller scale than the GHG emissions associated with direct electricity consumption.

Figures 3.12 and 3.13 show GHG emissions for the DCMB and Fort Irwin cooling towers, respectively. Fort Irwin had higher wastewater discharge per refrigeration ton of cooling than the Monterey Bay tower. The amount of wastewater discharge is dependent on the quality of the makeup water and the subsequent amount of mineral build-up.

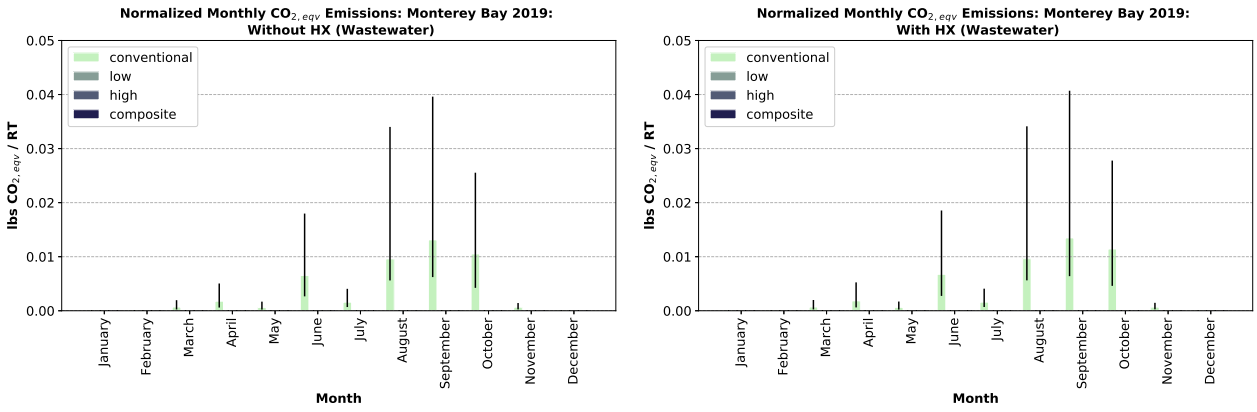

(a) Without Heat Exchanger (b) With Heat Exchanger

Figure 3.12: The monthly emissions (in $CO_{2,eqv}$) associated with wastewater discharged by the DoD Center Monterey Bay (DCMB) cooling tower in 2019 were normalized by refrigeration ton (RT) of the cooling tower capacity.

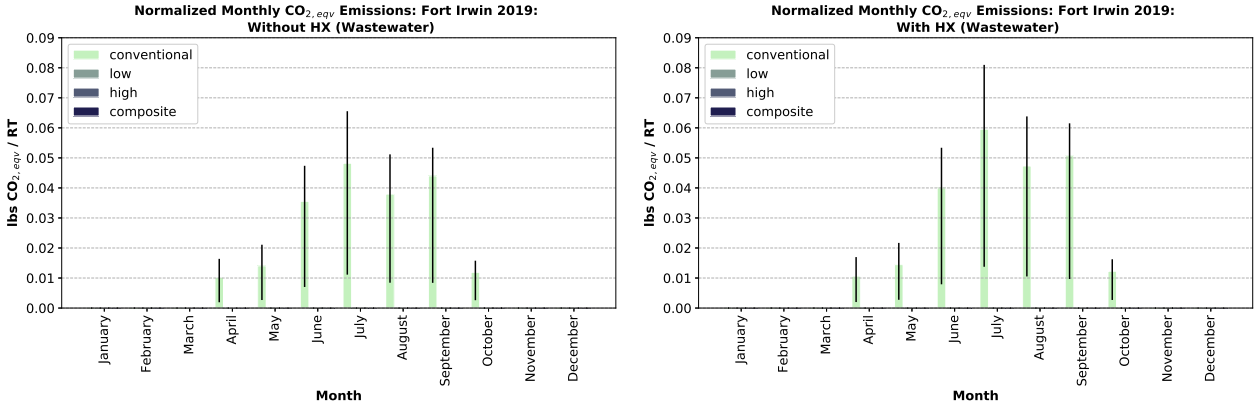

(a) Without Heat Exchanger

(b) With Heat Exchanger

Figure 3.13: The monthly emissions (in $CO_{2,eqv}$) associated with wastewater discharged by the Fort Irwin cooling tower in 2019 were normalized by refrigeration ton (RT) of the cooling tower capacity.

3.3.6 Monthly Greenhouse Gas Emissions Increase with respect to Water Savings

To further compare the tradeoff between water savings and increased GHG emissions, the increase of GHG emissions in pounds of CO_2 equivalents per gallon of water saved was calculated and is shown in Figures 3.14 and 3.15.

For the DoD Center Monterey Bay, the "hygroscopic low" mode had a significantly lower tradeoff between GHG emissions and water savings compared to the "hygroscopic high" and "hygroscopic composite" operations. In the moderate, coastal climate, the composite operational scenario had only a small improvement over the high scenario in terms of GHG emissions. This result is likely because the "hygroscopic composite" mode selected the best scenario in terms of sensible and latent cooling for the ambient air conditions, which fluctuate minimally in the Monterey Bay area.

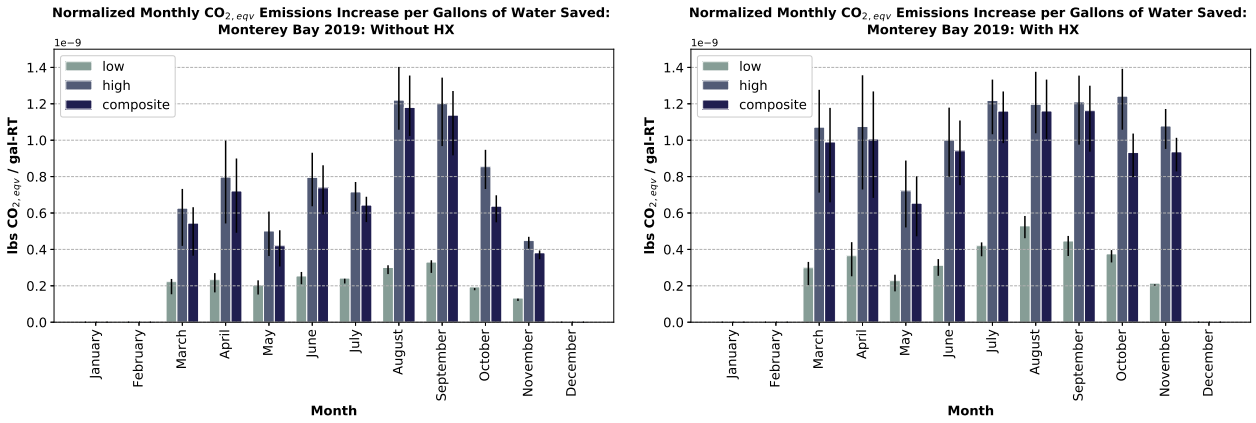

(a) Without Heat Exchanger (b) With Heat Exchanger

Figure 3.14: The total monthly emissions (in $CO_{2,eqv}$) increase per gallon of water saved by the hygroscopic cooling system at the DoD Center Monterey Bay (DCMB) cooling tower in 2019 were normalized by refrigeration ton (RT) of the cooling tower capacity.

At the Fort Irwin cooling tower, the "hygroscopic low" mode also had the lowest trade-off between GHG emissions and water savings; however, for the desert climate the composite operational scenario had only a slightly higher tradeoff than the low setting. The most aggressive water savings scenarios - "hygroscopic high" - had a relatively large tradeoff value because of the high electricity demands required to obtain water savings in the hot, arid climate.

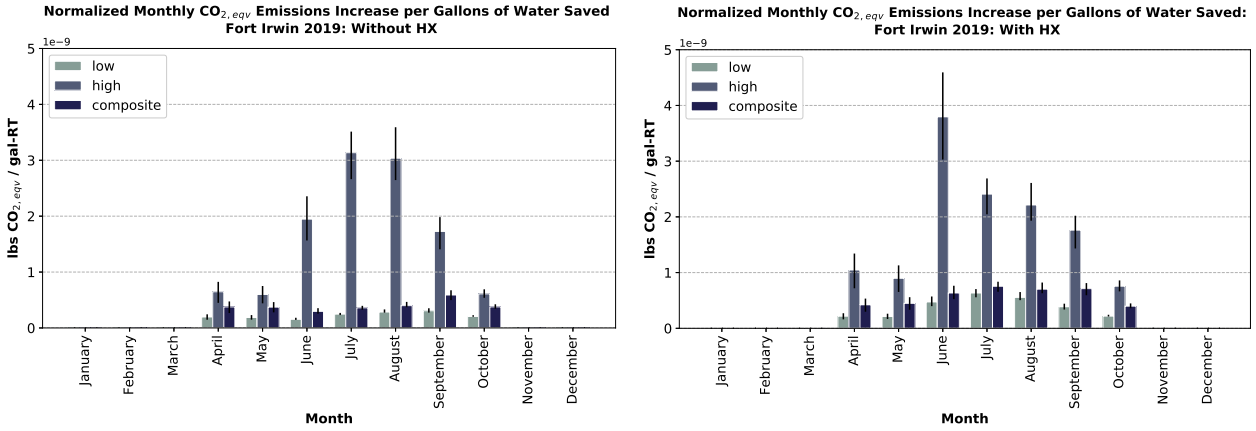

(a) Without Heat Exchanger (b) With Heat Exchanger

Figure 3.15: The total monthly emissions (in $CO_{2,eqv}$) increase per gallon of water saved by the hygroscopic cooling system at the Fort Irwin cooling tower in 2019 were normalized by refrigeration ton (RT) of the cooling tower capacity.

The optimal operational scenario depends on the operators' goals for water and energy savings, water availability, climate, and local water- and energy-savings requirements.

If the goal for the cooling system is to balance water savings and GHG emissions, then it would be advised to operate the hygroscopic system on the "low" water savings mode in both a coastal and a desert climate. However, in extremely water-scarce regions where water savings is a priority, it might make sense to operate the system on the "high" or "composite" setting, depending on the local air temperature and humidity.

3.3.7 Water Intensity Required for Zero-Emissions-Increase when switching from Conventional Evaporative Cooling to Hygroscopic Cooling

This analysis revealed that the GHG emissions associated with electricity generation far outweigh GHG emissions associated with water transport and treatment. To put this result into perspective, the energy intensity required for acquiring and treating water that would be necessary in a region to balance the current emissions from power production in California was calculated. The energy intensity value is in terms of electricity per million gallons of water (kWh/Mgal); this value refers to the weighted average of monthly water and wastewater treatment energy intensity.

Figures 3.16 and 3.17 show the minimum energy intensity for water and wastewater treatment required to reach zero-emissions-increase when switching from conventional evaporative cooling to hygroscopic cooling hygroscopic cooling system.

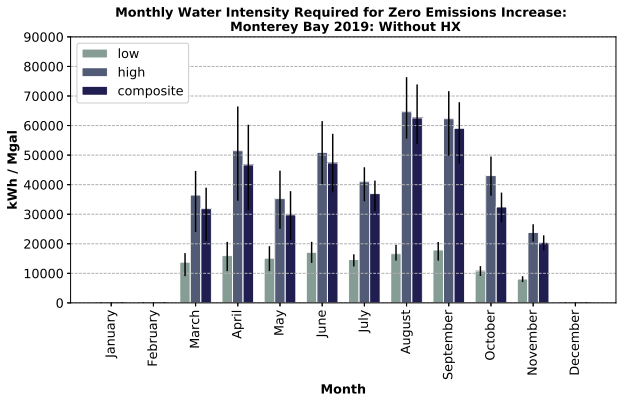

(a) Without Heat Exchanger

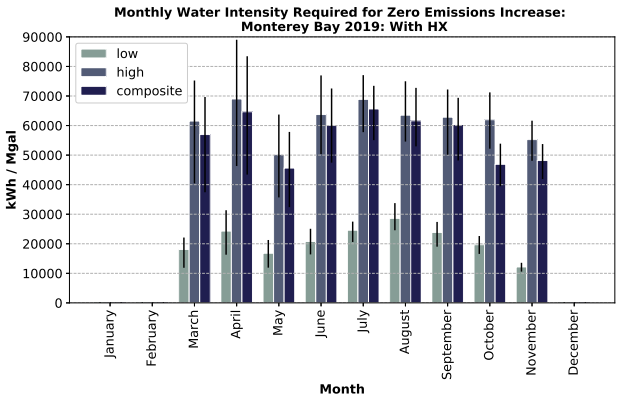

(b) With Heat Exchanger

Figure 3.16: The weighted average of monthly water and wastewater treatment energy intensity (in kWh per million gallon) required for there to be zero GHG emissions (in $CO_{2,eqv}$) increase associated with the switch to the hygroscopic cooling system for the DCMB cooling tower in 2019. The energy intensity of water is the weighted average of the energy required for sourcing, treating, and conveying water and the energy require for the conveyance and treatment of wastewater.

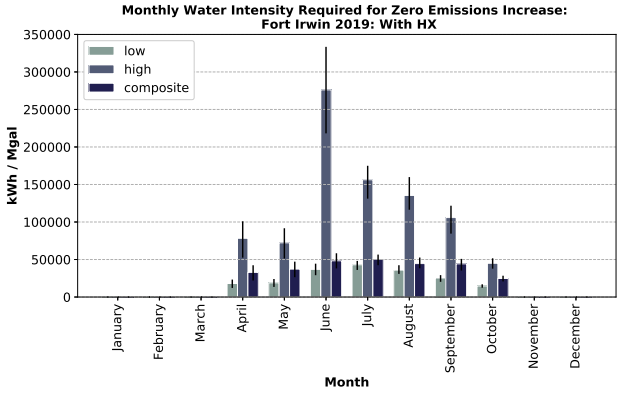

(a) Without Heat Exchanger

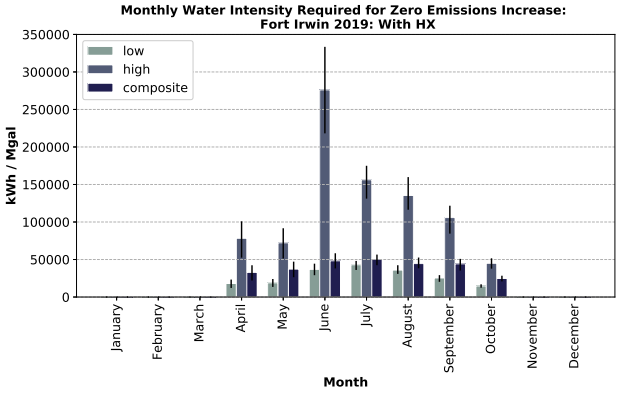

(b) With Heat Exchanger

Figure 3.17: The weighted average of monthly water and wastewater treatment energy intensity (in kWh per million gallon) required for there to be zero GHG emissions (in $CO_{2,eqv}$) increase associated with the switch to the hygroscopic cooling system for the Fort Irwin cooling tower in 2019. The energy intensity of water is the weighted average of the energy required for sourcing, treating, and conveying water and the energy require for the conveyance and treatment of wastewater.

The minimum water sourcing and treatment energy intensity required for zero-emissions-increase for the DCMB tower requires the "hygroscopic low" operational setting and ranges from about 12,160 kWh/Mgal to 28,590 kWh/Mgal and from about 8,080 kWh/Mgal to

17,920 kWh/Mgal for a system with and without a heat exchanger, respectively.

The minimum water sourcing and treatment energy intensity required for there to be no emissions increase for the Fort Irwin tower also requires the operation on the "hygroscopic low" mode. The values for this setting shown in Figure 3.17 range from about 14,750 kWh/Mgal to 43,000 kWh/Mgal and from about 13,700 kWh/Mgal to 20,820 kWh/Mgal for a system with and without a heat exchanger, respectively.

To put those values into perspective, the Seaside wastewater treatment plant reported embedded energy data for 2018 and 2019 that ranged from 953 kWh/Mgal to 1,631 kWh/Mgal (Figure 3.2). As previously stated, the drinking water treatment plant in the Marina Coast Water District in Seaside, CA, was estimated to use 1,453 kWh to source and treat one million gallons of water.

Based on a database of embedded energy for water and wastewater utilities from 2012, the embedded energy for water treatment in San Diego, CA, ranged from 507 kWh/Mgal to 770 kWh/Mgal; the embedded energy for wastewater treatment in San Diego, CA, ranged from 2,307 kWh/Mgal to 2,820 kWh/Mgal [28].

Southern California has the highest water sourcing, conveyance, and treatment energy in the United States [27]. Conveying water from northern California to southern California requires approximately 11,000 kWh/Mgal [27]. Desalination is the most energy-intensive water treatment method; desalination via reverse osmosis requires 13,200 – 26,500 kWh/Mgal [27].

For the current fuel resource mix for California's energy sector, reaching a zero-emissions-increase for the transition to the hygroscopic system is unlikely even with the most energy intensive water treatment methods. The electricity used for water sourcing, conveyance, and treatment and for operating the HVAC towers would need to come from low-carbon electricity sources to reduce GHG emissions overall. California currently has some of the lowest output emissions rates for electricity generation in the United States, and the CAMX eGrid sub-region that covers most of California is second only to NYUP (the Upstate NY eGrid sub-region) in terms of lowest pounds of $CO_{2,eqv}$ per MWh generated [12]. For the hygroscopic cooling tower to be more feasible from a GHG emissions standpoint, the electricity grid as a whole will need to make vast efforts to move towards low-carbon energy sources.

CHAPTER 4

DIRECT AND INDIRECT WATER CONSUMPTION AND WITHDRAWAL

4.1 Introduction

The water savings achieved by the hygroscopic cooling system come at the cost of increased cooling water usage for electricity generation. The increase in cooling water consumption can be compared to the evaporative water consumption by the HVAC cooling towers. However, unlike the cooling water used at the building scale, the cooling water at the electricity generation scale is not typically treated municipal drinking water. Therefore, the power generation cooling water does not have the same indirect electricity and GHG emissions associated with it as does the HVAC makeup water.

Comparing water consumption rates and volumes is a standard in literature; however, water withdrawal should not be completely ignored due to its adverse environmental impacts. Water returned to water bodies after use is often returned at a higher temperature and lower quality, which that negatively impacts the ecosystem.

Quantifying direct and indirect water usage incorporated the following research questions:

- What is the relationship between water savings at the building-scale cooling tower and water consumption at the power generation scale?
- How does an increase in electricity usage impact the volume of water withdrawal?

Cooling water withdrawal is responsible for killing billions of aquatic organisms annually [32]. Water withdrawals are the total volume of water entering intake structures, and this process is responsible for injuring and killing fish and other aquatic organisms. In California, 19 once-through cooling systems were responsible for killing approximately a dozen seals, two dozen sea lions, 2.7 million fish, and 19.4 billion larvae annually [33].

An increase in water temperature can make the habitat unlivable for some aquatic organisms due to temperature extremes and lower amounts of dissolved oxygen in the water. Cooling water discharge averages 37°C during summer months, which is a 9.5°C to 10.5°C increase with respect to original water temperature [34]. One review found that an increase of only 1°C can reduce the growth, development, and reproductive success of aquatic organisms by 10%, and an increase of 7°C can reduce these processes by 50% [35].

Once-through cooling systems are responsible for most of the elevated-temperature discharge back into bodies of water. Return flows reflect the water being returned to a body of water at a higher temperature and overall lower quality; these flows were excluded from this analysis.

4.2 Methods

For this analysis, monthly withdrawal and consumption values were gathered from the U.S. Energy Information Administration (EIA) data and estimated for plants without reported values in California from 2010-2018. There was a drought in California from 2011-2019 that affected the energy resource mix in the state [9]. Analyzing years throughout different stages of the drought provides a more accurate depiction of the monthly and annual variation in water withdrawal and consumption. Monthly withdrawal and consumption values were estimated for natural gas, nuclear, hydro, coal, and solar power plants; power generation facilities that use these fuel types have the most significant cooling water requirements.

4.2.1 EIA Data Availability

Form EIA-923 Schedule 8 provides limited data for power plant cooling water withdrawal and consumption. EIA-923 requires thermoelectric power plants with a total steam capacity greater than 100 megawatts to report monthly cooling data [36], including organically fueled, combined-cycle, and nuclear power plants. For this analysis, water consumption and withdrawal were estimated for natural gas, nuclear, and coal power plants with a capacity less than 100 megawatts and for hydropower and solar power generation.

Plants with once-through cooling systems will often report their water consumption as zero gallons. This data reporting ignores evaporative losses in once-through cooling systems and cooling ponds. In these cases, the reported withdrawal was used while consumption was estimated based on factors reported in literature [20].

Water consumption and withdrawal values reported as zero in EIA-923 were estimated using electricity generation data reported in EIA-923 and water consumption and withdrawal factors reported in literature [20, 23].

Using forms EIA-923 and EIA-860, California power plant data were sorted by fuel type, generation technology types, and cooling system type [15][37]. Once the data were sorted, water consumption and withdrawal factors were applied from literature [20] to obtain volumetric estimates for water use. For more accurate hydropower consumption estimates, net evaporation factors from Grubert were used [23]. Using water and electricity usage data from the cooling towers studied in this demonstration, water savings from building-scale cooling and the increase in water use for power plant cooling was directly compared.

4.2.2 Code Methodology

The process of sorting forms EIA-923 and EIA-860 and applying water consumption and withdrawal factors from literature is provided in the flowchart in Figure 4.1.

Form EIA-923 includes the plant ID, plant state, prime mover, reported fuel type, monthly electric fuel consumption (in MMBtu), and monthly net electricity generation (in MWh) [15]. The environmental equipment spreadsheet in Form EIA-860 provides cooling type information for natural gas plants, concentrated solar power, nuclear plants, and biopower plants. The EIA data were sorted in the following order: fuel type, prime mover, cooling type, and specific technology.

For natural gas power plants, cooling factors were assigned to combined-cycle plants for "Combined Cycle Steam Part", "Combine Cycle Single Shaft", and for steam turbines. Combustion turbines are not cooled by water and, therefore, were not included. Cooling water factors from Macknick et al. [20] break down into four different cooling types: tower, once-through, dry cooling, and pond. For natural gas generation stations, several plants do

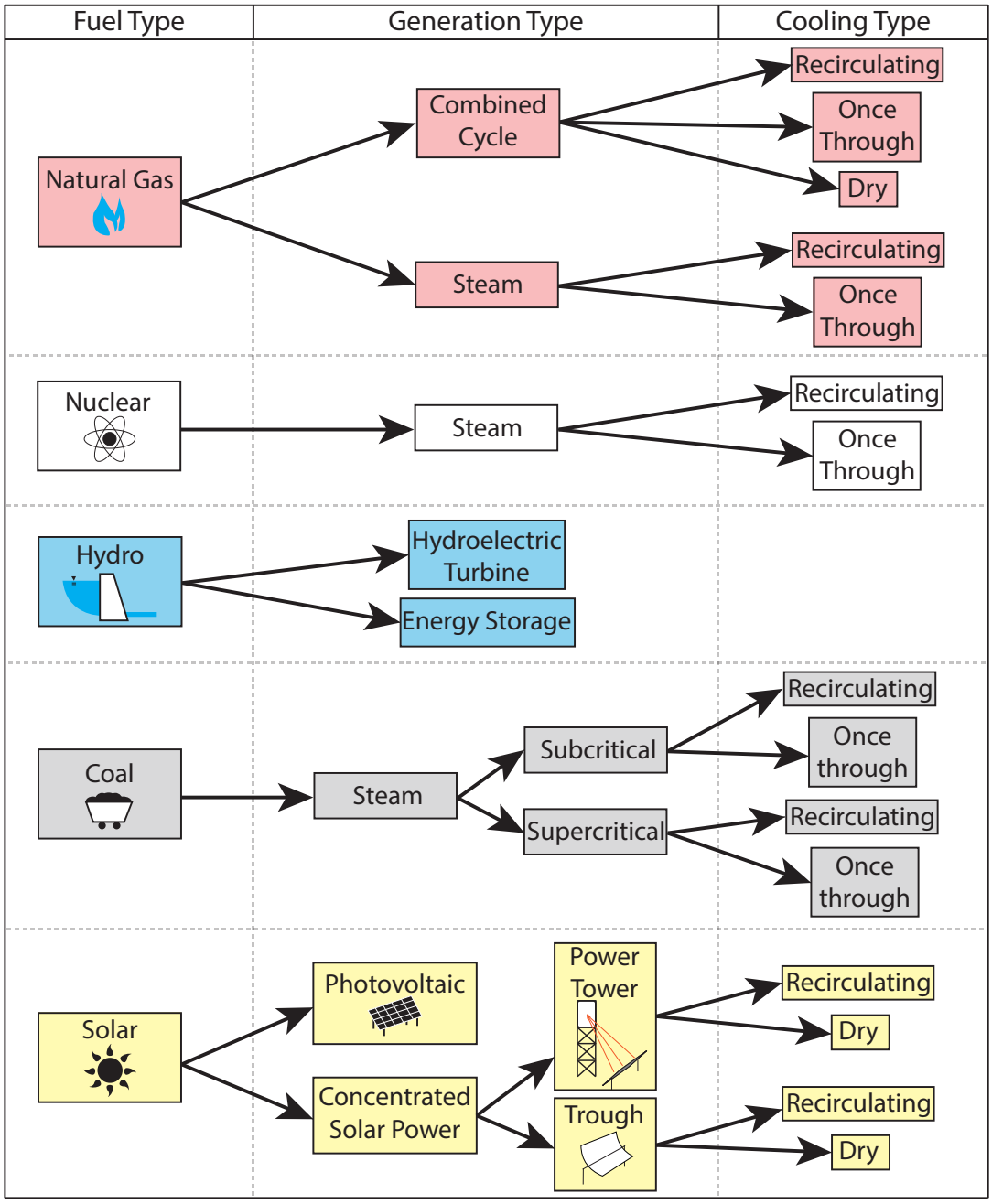

Figure 4.1: Water consumption and withdrawal was estimated based on EIA power plant data and Macknick et al.'s water usage factors [20] and Grubert's hydroelectric water usage study [23]. Form EIA-923 and EIA-860 provide data by plant. Plant data was sorted by fuel type, generation type, then cooling technology type. The fuel types included in this analysis are natural gas, nuclear, hydropower, coal, and solar power. Pond cooling systems were not present in California and were therefore not included in this graphic.

Table 4.1: Water consumption factors (gal/MWh) [20, 23].

Fuel Type	Generation Type	Cooling Type	Median	Min	Max
Natural Gas	Combined Cycle	Recirculating	205	130	300
		Once-Through	100	20	100
		Dry	2	0	4
	Steam Turbine	Recirculating	826	662	1170
		Once-Through	240	95	291
Nuclear	Steam	Recirculating	672	581	845
		Once-Through	269	100	400
Hydro	Hydroelectric Turbine		1585	1132	3491
	Energy Storage		1585	1132	3491
Coal	Subcritical	Recirculating	479	394	664
		Once-Through	113	71	138
	Supercritical	Recirculating	493	445	594
		Once-Through	103	64	124
Solar	Photovoltaic		1	0	5
Concentrated Solar Power	Power Tower	Recirculating	786	751	1109
		Dry	26	26	26
	Trough	Recirculating	906	725	1109
		Dry	78	43	79

not have cooling type reported. Only steam-electric plants with a nameplate of 100 MW or greater are required to report cooling data [38]. In instances where cooling type is not reported, it was assumed that a tower was used because cooling towers are more common in smaller power plants due to the space constraints and required cooling capacity. This data gap filling was supported by analyzing satellite photos of plants with missing cooling data.

Hydroelectric power plants are reported to the EIA as hydroelectric turbines and energy storage. Since hydroelectric power plants do not require cooling, Grubert's data on hydroelectric water consumption was used to estimate net evaporative losses in reservoirs [23]. Grubert takes an in-depth look at the water losses associated with seepage and evaporation in reservoirs used for hydropower and found hydropower net water consumption to be 1,585 gallons/MWh. This estimate is significantly lower than Macknick et al.'s estimation of 4,491 gallons/MWh for gross reservoir evaporation [20].

Solar power generation was divided into two categories: photovoltaic and concentrated solar power. Photovoltaic panels use minimal water for cleaning the panels. Concentrated

Table 4.2: Water withdrawal factors (gal/MWh) [20].

Fuel Type	Generation Type	Cooling Type	Median	Min	Max
Natural Gas	Combined Cycle	Recirculating	255	150	283
		Once-Through	11380	7500	20000
		Dry	2	0	4
	Steam Turbine	Recirculating	1203	950	1460
		Once-Through	35000	10000	60000
Nuclear	Steam	Recirculating	1101	800	2600
		Once-Through	44350	25000	60000
Coal	Subcritical	Recirculating	587	463	714
		Once-Through	27088	27046	27113
	Supercritical	Recirculating	634	582	670
		Once-Through	22590	22551	22611
Solar	Photovoltaic		1	0	5
Concentrated Solar Power	Power Tower	Recirculating	786	751	1109
		Dry	26	26	26
	Trough	Recirculating	906	725	1109
		Dry	78	43	79

solar power is a broad term for a range of solar technologies that use a steam turbine. EIA-860 provides details about the type of concentrated solar power (CSP) being used. These technologies include parabolic trough, linear Fresnel, power tower, and dish engine. As of 2018 in California, the only reported CSP technologies in use were parabolic trough and power tower. These technologies are cooled by induced draft towers and dry cooling systems. For plants with missing data, satellite images were used to identify and assign the cooling type.

Nuclear power plants use steam for electricity generation and use one of the following cooling technologies: tower, once-through, or pond. Based on the cooling code from EIA-860, the plants were sorted into one of these three cooling types. By 2018, California only had one operational nuclear power plant — the Diablo Canyon Plant [15].

Coal power plants were also sorted based on the three common wet-cooling types: tower, once-through, and pond. EIA-860 includes details about the plant system technologies including subcritical technology, supercritical technology, and carbon capture and storage technology (CCS). Supercritical boilers operate at higher pressures than subcritical systems.

Subcritical and supercritical systems with CCS technology consume more water than their conventional counterparts. By 2018, California only had one operating coal power plant left — the Argus Cogen Plant [15].

Once water withdrawal and consumption quantities were estimated, the monthly and annual fluctuations in cooling water use were compared. The tradeoff between reducing water use in building-scale cooling and the increase in power plant cooling water associated with that operational change were quantified.

4.3 Results

The results of the analysis are divided into four sections — consumption and withdrawal factors, total direct and indirect water consumption by the building-scale cooling system, consumption volumes, and withdrawal volumes. Average monthly consumption and withdrawal factors for California were determined in the first section to calculate water consumption and withdrawal volumes associated with the building-scale systems. Visualizations of the monthly consumption and withdrawal factors from 2010 to 2018 provide insight into how water usage at the power plant level has changed throughout the time span of the drought.

Water consumption and withdrawal volumes were calculated for four different scenarios — conventional wet cooling, hygroscopic low, hygroscopic high, and hygroscopic composite. Water consumption at the power generation scale was also compared to the consumption at the building scale.

Water withdrawal at the power generation scale was calculated in addition to consumption values, even though it is not used in the comparison of direct and indirect water use associated with the building cooling tower. Water withdrawal volumes are included due to its impact on aquatic environments.

4.3.1 Withdrawal and Consumption Factors

Water consumption and withdrawal factors for California from 2010 to 2018 were used to convey the temporal variation in water usage factors. It is beneficial to compare how the

factors vary both monthly and annually.

Box plots were produced to clearly display the median values and annual distribution of the monthly factors. Line graphs were produced to simultaneously visualize the wide monthly and annual variation that cannot be ascertained from the box plots.

Figure 4.2 illustrates this wide variation of monthly consumption factors from month-to-month and from year-to-year. Each grey line represents a year from 2010-2018; 2010 is represented by the darkest grey line, and 2018 is represented by the lightest grey line. The red dashed line depicts the monthly average for 2010-2018. The monthly average was used for estimating indirect consumption throughout this analysis.

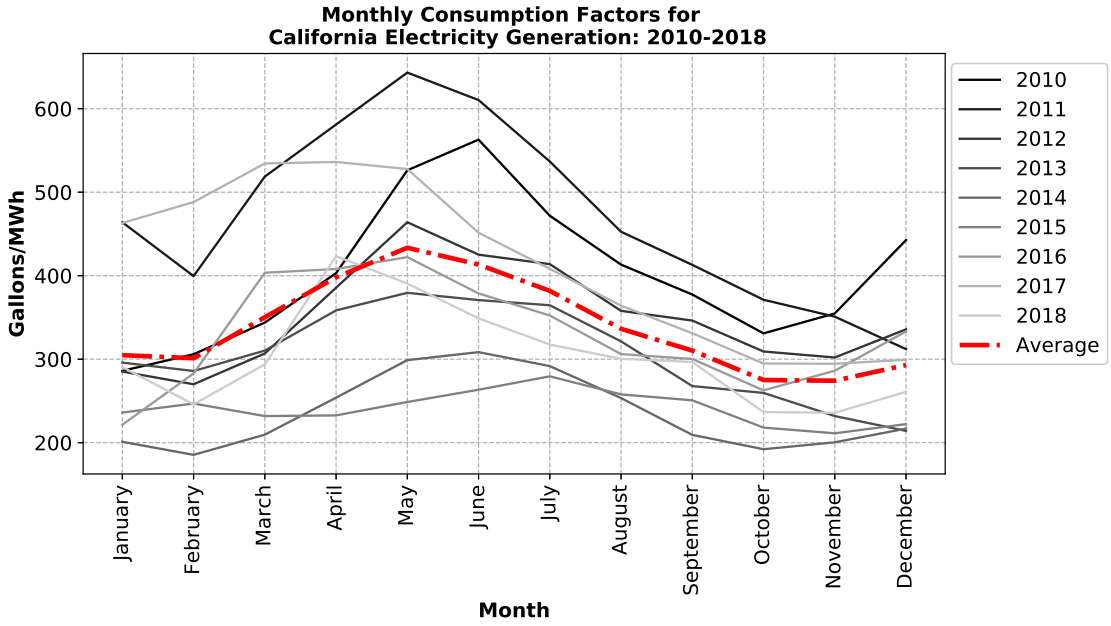

Figure 4.2: Monthly cooling water consumption factors for California electricity generation from 2010 to 2018 varies monthly and annually. Each grey line represents a year from 2010-2018; 2010 is represented by the darkest grey line and 2018 is represented by the lightest grey line. The red line represents the average monthly factors for the nine-year span.

California experienced a drought from 2011 until 2019 [9]. Droughts change the composition of a region's energy resource mix, which contributes to the wide temporal variation in consumption factors. During periods of drought, California switches some energy production from hydropower to natural gas [12]. In general, water consumption increased as drought conditions lessened.

This increase in consumption is likely due to efforts to decrease the negative impacts on aquatic ecosystems by once-through cooling systems [39], along with the increase of hydropower production as drought conditions improved. Wet-cooling towers consume more water than once-through cooling systems, while once-through cooling systems withdraw more water.

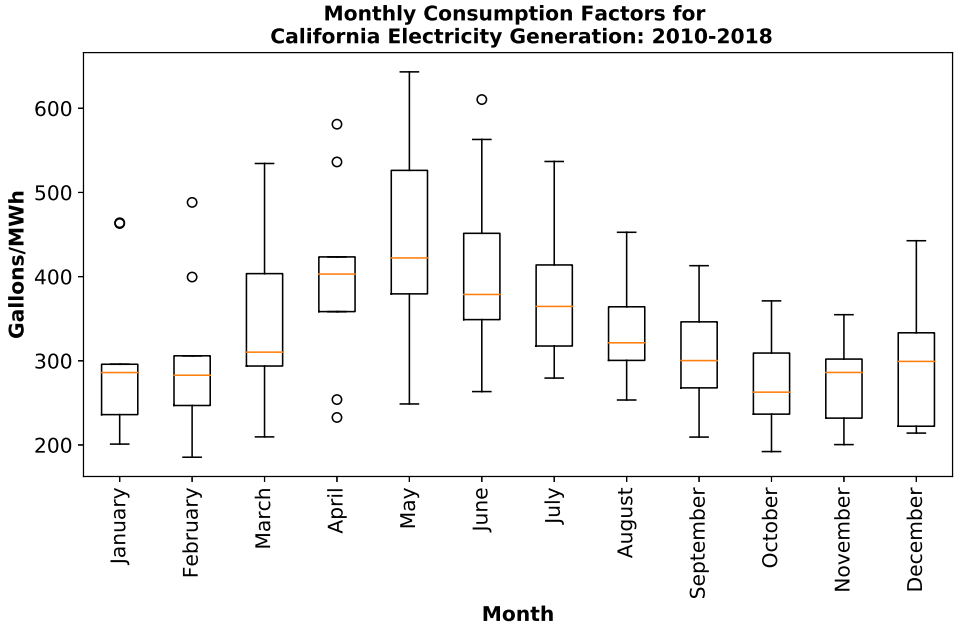

Figure 4.3: Monthly cooling water consumption factors for California electricity generation from vary over the analysis time of 2010-2018.

Figure 4.3 shows the monthly consumption factors for California in closer detail. The greatest range in consumption factors occurs from March to June with standard deviations of 107.1 gal/MWh in April to 115.3 gal/MWh in May.

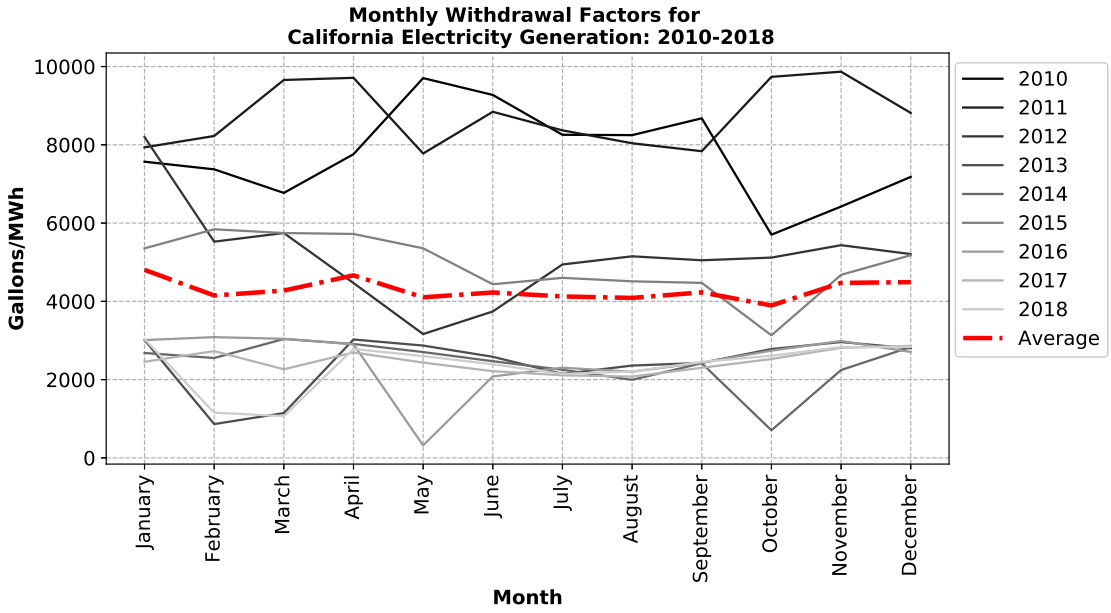

Figure 4.4: Monthly cooling water withdrawal factors for California electricity generation from 2010 to 2018 varies monthly and annually. Each grey line represents a year from 2010-2018; 2010 is represented by the darkest grey line and 2018 is represented by the lightest grey line. The red line represents the average monthly factors for the nine-year span.

The monthly withdrawal factors also varied greatly on both monthly and annual scales. Each grey line represents a year from 2010-2018; 2010 is represented by the darkest grey line, and 2018 is represented by the lightest grey line. The dashed red line depicts the monthly average from 2010-2018. The monthly average was used for estimating volumetric withdrawal associated with the HVAC cooling towers throughout this analysis.

From 2010 to 2018, there has been a general decrease in the monthly withdrawal factors. This matches the increase in consumption factors associated with the phasing out of once-through systems and the increase in hydropower operation with the improvement of drought conditions.

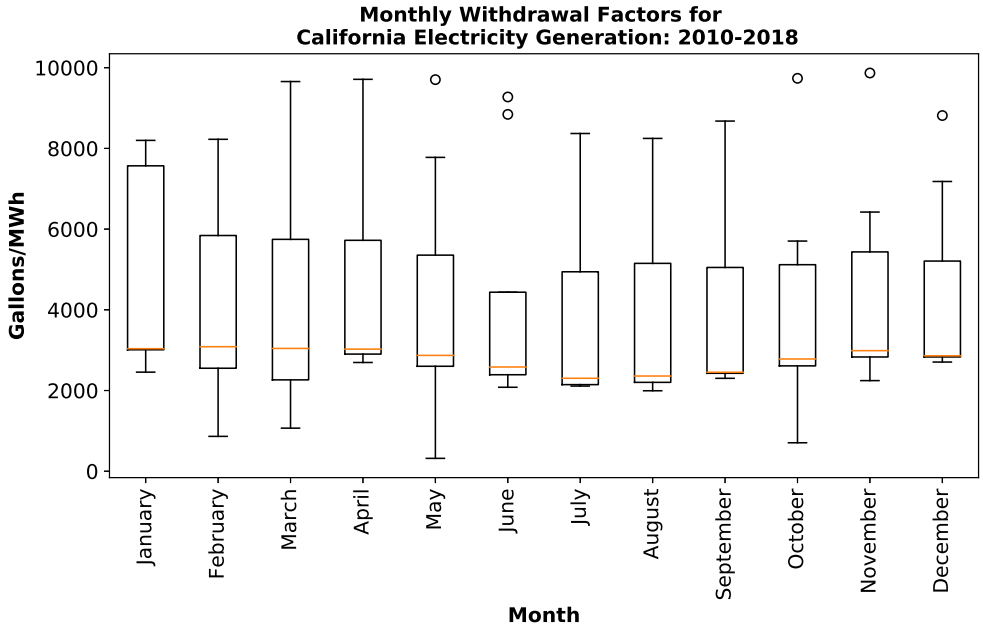

Figure 4.5: Monthly cooling water withdrawal factors for California electricity generation vary over the analysis time of 2010-2018.

Monthly water withdrawal factors varied consistently throughout the year for California's power sector from 2010-2018. The greatest variation from year-to-year occurred during the late winter and spring months.

The greatest monthly ranges in withdrawal factors occurred from February to June with standard deviations of 2,415 gal/MWh in April to 2,792 gal/MWh in May. Spring months had the highest standard deviations, likely due to the variation in snowmelt coming from the mountains in the spring and the subsequent amount of electricity generated by hydropower plants [31]. Monthly averages were used to estimate monthly volumetric water withdrawal.

4.3.2 Direct versus Indirect Water Usage

Total direct water usage by the building cooling system is the sum of the evaporated makeup water and the wastewater that flushes mineral concentrations to the sewer. Direct water consumption refers to makeup water evaporated by the building HVAC cooling system. The abbreviation "CD" represents "Consumption – Direct", or the evaporated makeup water. The abbreviation "SD" represents "Sewer – Direct", or the blowdown from

the conventional wet-cooling tower. Direct water usage is represented in the following figures (Figure 4.6 and 4.7) as shades of green — the lighter shade represents direct blowdown and the darker shade represents direct evaporative consumption.

Indirect water consumption refers to the water consumption associated with the cooling water required for generating the electricity used directly by the building HVAC cooling tower. Indirect water consumption is a combination of reported data from Form EIA-923 and estimated using cooling water consumption factors from literature. The abbreviation "CI" refers to "Consumption – Indirect" and is represented by the blue bars at the bottom of the visualizations in Figures 4.6 and 4.7.

In the stacked bar graphs in Figures 4.6 and 4.7, each bar in the grouping corresponds with one of the building-scale cooling towers' operational modes — conventional wet cooling, "hygroscopic low", "hygroscopic high", and "hygroscopic composite". The conventional wet cooling tower water usage is the first bar in the grouping without any texture applied. The "hygroscopic low" scenario is the second bar and is textured with angled stripes. The "hygroscopic high" scenario is the third bar in the grouping and is textured with dots. The final bar in each grouping conveys the values for the "hygroscopic composite" scenario and is textured with horizontal lines.

Indirect water consumption (CI) is comparatively small in relation to direct water consumption (CD). The hygroscopic system is effective in reducing water use even when factoring in the indirect water consumption at the power generation scale. The "hygroscopic high" and "composite" operational modes have the best water savings results for the DCMB site. The "hygroscopic low" and "composite" operational modes have the best water savings results for a tower without a heat exchanger for the Fort Irwin site, while "hygroscopic composite" has the best savings for a tower that utilizes a heat exchanger. However, these water savings come at the cost of increased greenhouse gas emissions. Power generation-related water consumption is relatively low compared to building-scale water consumption, and therefore has a negligible effect on the total water savings.

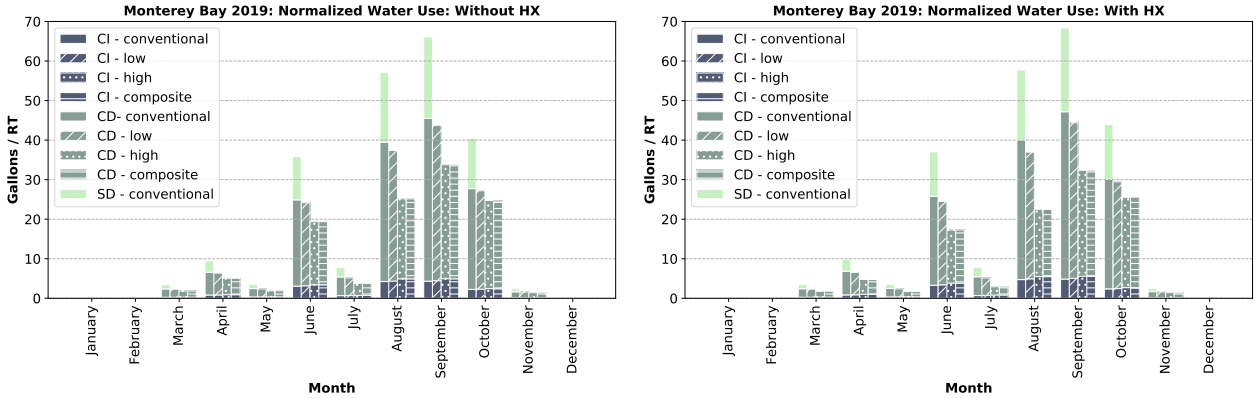

(a) Without Heat Exchanger

(b) With Heat Exchanger

Figure 4.6: The monthly direct and indirect water usage by the DoD Center Monterey Bay (DCMB) cooling tower in 2019 was normalized by refrigeration ton (RT) of the cooling tower capacity. Total direct and indirect water usage is the sum of indirect consumption associated with electricity use (CI), direct consumption (CD), and direct wastewater discharged to the sewer (SD).

The hygroscopic cooling system was successful in decreasing in reducing water consumption at the DCMB, even when factoring in indirect water consumption for electricity generation (Figure 4.6). However, at Fort Irwin total direct and indirect evaporative water consumption is actually greater for the hygroscopic system during peak operational months. It is when the reduction in water usage from eliminating blowdown is factored in that water savings are seen at Fort Irwin (Figure 4.7).

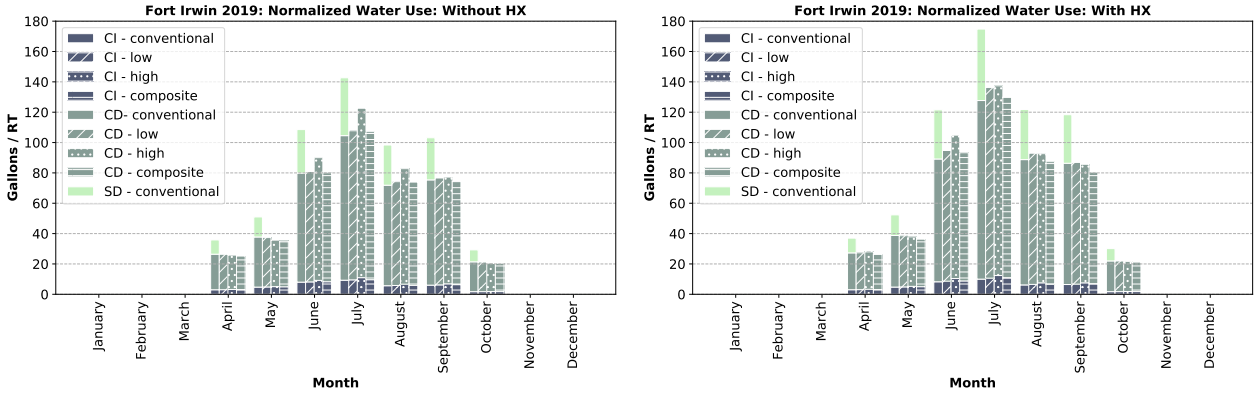

(a) Without Heat Exchanger

(b) With Heat Exchanger

Figure 4.7: The monthly direct and indirect water usage by the Fort Irwin cooling tower in 2019 was normalized by refrigeration ton (RT) of the cooling tower capacity. Total direct and indirect water usage is the sum of indirect consumption associated with electricity use, direct consumption (CD), and direct wastewater discharged to the sewer (SD).

In Section 3.3.6, it was determined that based on the tradeoff between increased GHG emissions and water savings, the "hygroscopic low" scenario was the best option for the arid climate of Fort Irwin, and "hygroscopic composite" had the second lowest tradeoff. Based on this finding and the data visualization in Figure 4.7, "hygroscopic low" is likely the best scenario for hygroscopic towers without the heat exchanger and "hygroscopic composite" is likely the best scenario for hygroscopic towers with the heat exchanger in the Fort Irwin climate.

4.3.3 Indirect Water Consumption

Indirect water consumption in this context refers to the water evaporated at the power plant to provide cooling during electricity generation. The goal of the hygroscopic cooling system demonstration was to decrease direct water consumption by the building cooling tower in comparison to conventional wet cooling. However, direct water savings comes at the cost of additional indirect water consumption due to increased electricity requirements for operating the novel hygroscopic system. The data in Figures 4.8 and 4.9 show the indirect water consumption increase associated with power generation for all four building cooling scenarios and for each scenario with and without a heat exchanger.

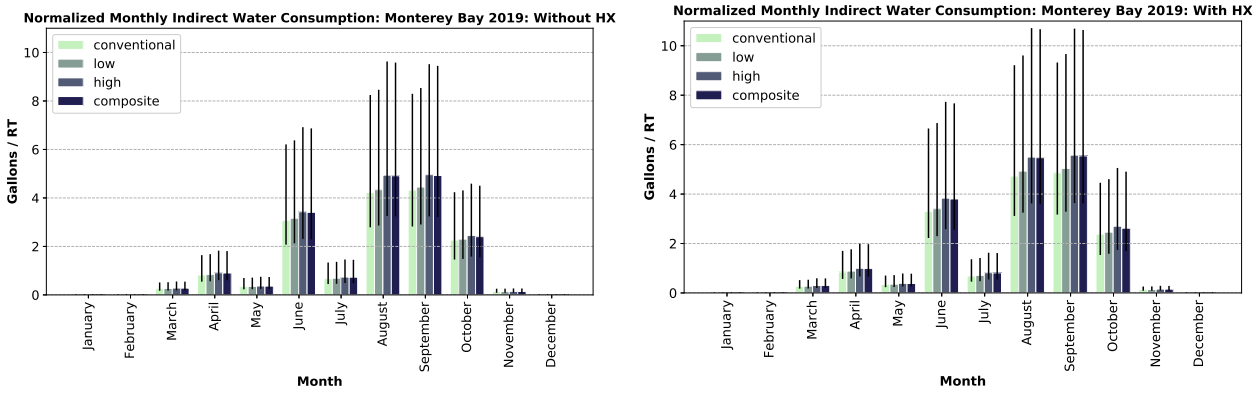

(a) Without Heat Exchanger (b) With Heat Exchanger

Figure 4.8: The monthly indirect water consumption by the DoD Center Monterey Bay (DCMB) cooling tower in 2019 was normalized by refrigeration ton (RT) of the cooling tower capacity.

The data processed to include the heat exchanger lead to higher water consumption due to performance losses resulting from the temperature increase in the condenser. The conventional cooling system has the lowest electricity consumption and therefore directly corresponds to lower indirect water consumption associated with electricity generation.

At the DCMB site, the "hygroscopic low" scenario is relatively similar to the conventional system, while "hygroscopic high" and "hygroscopic composite" lead to a greater water consumption increase.

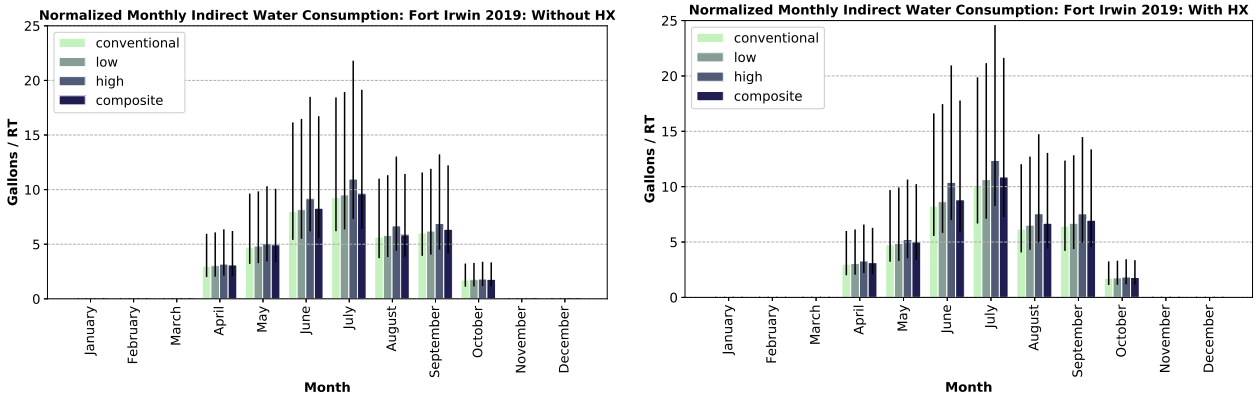

(a) Without Heat Exchanger (b) With Heat Exchanger

Figure 4.9: The monthly indirect water consumption by the Fort Irwin cooling tower in 2019 was normalized by refrigeration ton (RT) of the cooling tower capacity.

At the Fort Irwin demonstration site, the "hygroscopic low" scenario is relatively similar

to the volume of water consumption associated with the conventional wet cooling system. The "hygroscopic high" scenarios lead to the greatest water consumption increase. Fort Irwin requires significantly higher water consumption compared to the DCMB due to the high daytime temperatures.

Although the indirect water consumption is relatively low compared to direct water consumption, it illustrates how operating a cooling tower, or any technology that consumes electricity, in one location can affect water availability in another region. In some cases, electricity can be generated in regions with relatively low water scarcity, and in others, electricity generation might exacerbate water quantity and quality challenges in certain regions.

4.3.4 Indirect Water Withdrawal

When evaluating indirect water use associated with the building cooling system in Section 4.3.2, only the water consumed by the power plant was considered. While water withdrawal was not used to compare the indirect and direct water usage in Section 4.3.2, water withdrawal has a non-negligible environmental impact. Return flow from power plants is discharged at a lower quality and higher temperature, which affects aquatic organisms. In Figures 4.10 and 4.11, indirect water withdrawals are provided.

Regulations govern the temperature and quality of cooling water discharged from power plants; cooling water discharge temperatures are regulated by permits from the National Pollution Discharge Elimination System (NPDES). Water withdrawals for cooling power plants and manufacturing and industrial facilities are regulated under the Clean Water Act (CWA). Section 316(b) of the CWA issues guidelines for facilities that withdraw more than 2 million gallons per day and use 25 percent or more of that water for cooling purposes [32].

Water withdrawal was calculated to evaluate the impact of electricity usage on aquatic environments and to convey the environmental tradeoff of reducing building-scale cooling tower water consumption.

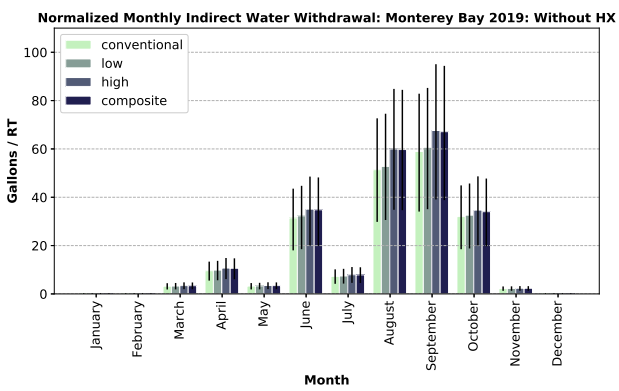

(a) Without Heat Exchanger

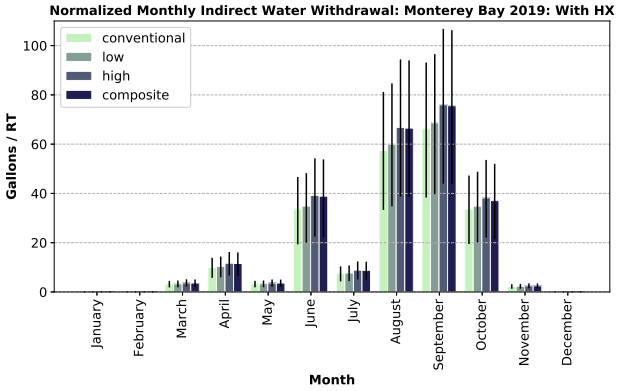

(b) With Heat Exchanger

Figure 4.10: The monthly indirect water withdrawal by the DoD Center Monterey Bay (DCMB) cooling tower in 2019 was normalized by refrigeration ton (RT) of the cooling tower capacity.

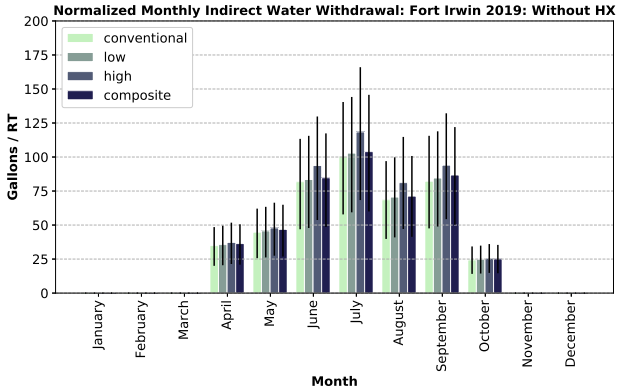

(a) Without Heat Exchanger

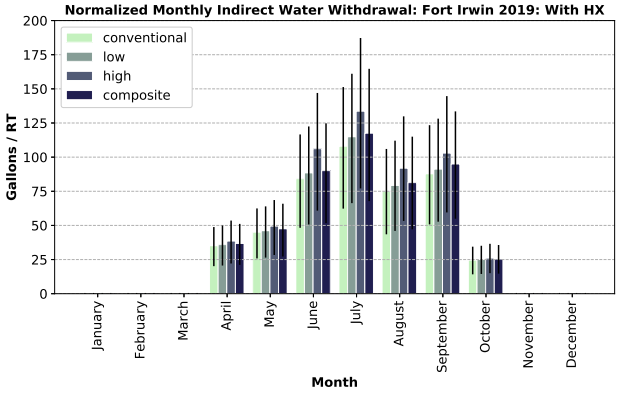

(b) With Heat Exchanger

Figure 4.11: The monthly indirect water withdrawal by the Fort Irwin cooling tower in 2019 was normalized by refrigeration ton (RT) of the cooling tower capacity.

The raw, non-normalized versions of the figures in this chapter are provided in Appendix B, along with the normalized and non-normalized water usage figures for Fort Irwin's HVAC cooling tower operation in 2018.

CHAPTER 5

IMPLICATIONS AND BROADER DISCUSSION

5.1 Discussion

The goal of the ESTCP hygroscopic cooling system demonstration was to "improve the tradeoff between water consumption and cooling efficiency in cooling towers used for heat rejection from various processes, including building heating, ventilation, and air conditioning (HVAC) loads; data center cooling; power generation; and various other industrial purposes" [6]. The DoD has estimated that there are over 4,000 individual cooling towers among Air Force, Navy, Marines, and Army facilities [6].

HVAC wet-cooling towers are significant water consumers and reducing their water consumption is an opportunity for water savings not only across DoD facilities, but across multiple sectors. HVAC cooling towers are common equipment at office buildings, large residential complexes, data centers, schools, and hospitals.

Although water scarcity is most severe in the western United States, streamflow and groundwater depletion is a growing concern across the country [40]. Reducing water demand is an important step to increase resilience in a warming world [41]. However, when the water savings comes at the cost of increased GHG emissions, the tradeoffs and the context of the application must be weighed carefully.

The effects of climate change are a series of interconnected consequences and feedback loops. Anthropogenic greenhouse gas emissions — such as those associated with HVAC cooling towers due to direct and indirect electricity consumption — are responsible for trapping heat in the atmosphere. Higher temperatures, especially in urban areas, increase the demand for cooling technology [42–44]. Climate change is also leading to an increase in regions facing water scarcity and the amount of land affected by drought [2]. This water

scarcity affects not only the availability of water for cooling purposes, but it also increases the cost and energy intensity for sourcing, conveying, and treating water for use in cooling systems. Higher energy intensity water and wastewater treatment methods, such as reverse osmosis and other desalination methods, are required for treating saltwater, and chemicals and pharmaceuticals in wastewater. In addition, saltwater intrusion is an increasingly frequent challenge due to the over withdrawing of water from aquifers [45]. Reverse osmosis is also frequently used for treating wastewater for direct potable water reuse [46].

Decarbonizing the power sector holds the greatest potential for mitigating the negative environmental impacts of building cooling. The extraction methods for coal and natural gas fuels, including mountaintop removal and hydraulic fracturing, introduce additional environmental hazards beyond GHG emissions [47, 48].

One 2011 study estimated that obtaining natural gas through hydraulic fracturing contributes 30-50% more methane emissions than conventional natural gas drilling [48]. As of 2015, the EIA reported that 67% of natural gas wells in the United States were hydraulically fractured wells [49]. This increase in hydraulically fractured natural gas wells raises additional environmental concerns because methane has a a global warming potential 25 times that of carbon dioxide.

EPA emissions factors, used for estimating GHG emissions associated with California's power sector in this study, are based on average emissions for various combustion methods for each fuel type; the EPA does not provide uncertainty information for their emissions factors [50]. Emissions that occur during the mining, processing, transportation, and storage of these fuels are not included in the EPA's emissions factors, and are therefore beyond the scope of this study. However, these emissions should not be completely ignored.

Nor should the impact of fossil fuel extraction on water usage and pollution be ignored. In terms of coal mining, surface mining uses a median of 3.2 m^3 of water per TJ of energy and underground mining uses 28.4 m^3 of water per TJ [16]. Natural gas drilling uses 1.1 m^3/TJ, while shale gas fracturing uses 12.6 m^3/TJ [16].

The future feasibility of beneficial hygroscopic cooling system installations is dependent on a number of factors, including the fuel source and extraction methods for electricity generation and the source and quality of water and its subsequent treatment requirements.

The ESTCP demonstration showed a limited scope of how the hygroscopic technology performs in different climates. While the system performed differently in each climate in terms of the increase of electricity consumption and the most favorable operational scenario, the system was successful in reducing water usage in both demonstration sites.

The hygroscopic cooling technology shows promising water savings ability that will likely be more feasible in regions with extreme water scarcity, high water sourcing and treatment energy intensity, and/or when the electricity is sourced from low-carbon sources.

5.2 Limitations and Uncertainty

The analysis of conventional wet cooling and the hygroscopic cooling systems was limited by the length of operation for each of the four scenarios. In the ESTCP demonstration, the hygroscopic system was integrated into an existing wet-cooling tower to compare both technologies and allow the conventional system to continue to carry most of the buildings' cooling load. The heat exchanger was needed to retrofit the existing system, connecting the working fluid in the hygroscopic cooling tower to fluid in the chiller responsible for the buildings' cooling load. A newly constructed hygroscopic cooling tower would not need this efficiency-loss inducing heat exchanger. Throughout the demonstration period, each scenario (conventional cooling, hygroscopic low, hygroscopic high, and hygroscopic composite) was only tested a fraction of the time. The data for each scenario was later processed as if each had run 100% time to allow for comparison and insight on total water and electricity usage. Due to this method of testing, there is error in the water and electricity data reported from the cooling tower because each testing scenario was run during a different time of day and varying ambient weather conditions.

The demonstration in Fort Irwin lasted from 2018 to 2019, and the demonstration in Monterey lasted throughout 2019. At the time of this analysis in May 2020, EIA power plant data were available until 2018. It was decided to use an average of energy data from a span of years rather than only the data from 2018 and 2019 during the demonstration period. The goal of this analysis was not to provide water consumption and withdrawal volumes for the specific time period of the demonstration, but to analyze the performance of the hygroscopic

system in different climates. The average water consumption and withdrawal factors based on 2010-2018 data were used to factor in the monthly and yearly variation in power plant operations due to weather patterns, electricity generation legislation, and extreme events (e.g., drought).

For the sake of this analysis, GHG emissions factors and indirect cooling water factors were calculated for California only, and GHG emissions and cooling water associated with imported and exported electricity were not considered.

5.2.1 Greenhouse Gas Inventory

The uncertainty values surrounding GHG emissions related to makeup water use and wastewater discharge are relatively large because the data for the energy requirements for water sourcing, treatment, and conveyance are both limited and laborious to attain. Unlike energy data reported to the EIA, there is not an extensive publicly available database of water utility data. A 2012 HydroShare database exists for over 160 utilities [28], reporting energy data that were acquired from 73 water and 90 wastewater facilities in major urban areas. The assembled data were acquired via open data requests to individual utilities across the United States and are therefore dependent on what each utility had available and the cooperation of each utility.

The uncertainty was propagated using a min-max method based on mean values and standard deviations, based on the data reported in the HydroShare database [25]. These data are for all of the United States, not just California, which increases uncertainty.

5.2.2 Indirect Water Consumption and Withdrawal

The analysis of indirect water consumption and withdrawal was limited by the lack of reported cooling water consumption and withdrawal data. Form EIA-923 only requires power plants with a total steam nameplate capacity greater than 100 MW to report cooling water data [36]. These reported data include natural gas, nuclear, and coal generators. The cooling water reported by Macknick et al. have varying uncertainty and limited sample sizes

associated with them [20]; however, these data represent the best available values to fill gaps in EIA reported values. Uncertainty was propagated for all generating units that did not have reported data, including thermoelectric power plants with a nameplate capacity less than 100 MW, hydropower plants, and solar power generation.

CHAPTER 6

CONCLUSION

The goal of this analysis was to quantify how novel hygroscopic cooling systems at two ESTCP demonstration locations in California affected greenhouse gas emissions and indirect water usage.

The following research questions were answered for the ESTCP hygroscopic cooling system demonstration:

What are the GHG implications of switching from a conventional wet cooling system to a hygroscopic system?

- What are the specific GHG implications of water conservation at the sites of interest?

  The impact of increased electricity use on GHG emissions is greater than energy savings from decreasing water demand. GHG emissions increased greatly when switching from conventional wet cooling to hygroscopic cooling at Fort Irwin and the DCMB in Monterey Bay. Dry cooling systems use more electricity than wet cooling systems, and hygroscopic cooling might be a better option in terms of GHG emissions than dry cooling.

- Are there locations with unrecognized potential for GHG reductions through water conservation? How might future water source alternatives (e.g., inland desalination) impact GHG projections?

  For the switch to the hygroscopic system to reduce GHG emissions, the energy intensity of the source water would have to exceed the reported energy intensity of water in the United States. Such water sources would have to be transported extremely long distances and/or treated with energy-intense operations such as desalination. Low-carbon electricity sources could similarly reduce the GHG emissions associated with

hygroscopic cooling systems. In this analysis, GHG emissions were estimated using California power plant data. CAMX, the eGRID sub-region that contains most of California, has the second lowest GHG emission output rate in the United States [12]. However, the generation resource mix of the U.S. grid might include higher percentages of low-carbon fuel types in the future.

How do water savings at a building-scale affect water usage at the power generation scale?

- The general trends in California from 2010-2018 show that cooling water consumption factors have increased while cooling water withdrawal factors have decreased.
- When compared to the volume of direct water usage that is reduced by switching from conventional wet cooling to the hygroscopic system, the indirect water consumption is comparatively low.
- The hygroscopic cooling technology is effective in reducing overall water consumption, despite the fact that indirect water consumption and withdrawal are greater for the hygroscopic cooling system due to the increase in electricity required for operations.

This reduction in water consumption comes at the cost of increased water withdrawal for electricity generation and an increase in greenhouse gas emissions associated with direct and indirect electricity use.

The hygroscopic cooling system is a promising technology in regions of high water scarcity and/or low-carbon electricity sources. Water scarcity is a growing concern worldwide [5], severe droughts are becoming more common, and the future might realize a less carbon-intense electricity grid. Scenarios were the hygroscopic cooling technology are beneficial might continue to increase as climate change worsens and as the power sector continues to move towards low-carbon energy sources.

CHAPTER 7

REFERENCES

[1] J. Rockström, W. Steffen, Kevin Noone, Åsa Persson, F Stuart Chapin III, E.F. Lambin, T. Lenton, M. Scheffer, Carl Folke, Hans Schellnhuber, Björn Nykvist, Cynthia de Wit, Terence Hughes, Sander Van der Leeuw, H. Rodhe, Sverker Sörlin, P. Snyder, Robert Costanza, Uno Svedin, and J. Foley. A safe operating space for humanity. *Nature, v.461, 472-475 (2009)*, 46, 01 2013.

[2] Bryson Bates, Z.W. Kundzewicz, S. Wu, V. Burkett, Petra Doell, D. Gwary, C. Hanson, B. Heij, Blanca Jiménez, G. Kaser, A. Kitoh, S. Kovats, P. Kumar, C.H.D. Magadza, D. Martino, Luis Mata, Mahmoud Medany, Kathleen Miller, and Nigel Arnell. Climate Change and Water. Technical Paper of the Intergovernmental Panel on Climate Change. 06 2008.

[3] William Cosgrove and Pete Loucks. Water management: Current and future challenges and research directions. *Water Resources Research*, 51, 06 2015. doi: 10.1002/2014WR016869.

[4] Robert McDonald, Pamela Green, Deborah Balk, Balazs Fekete, Carmen Revenga, Megan Todd, and Mark Montgomery. Urban Growth, Climate Change, and Freshwater Availability. *Proceedings of the National Academy of Sciences of the United States of America*, 108:6312–7, 03 2011. doi: 10.1073/pnas.1011615108.

[5] Matti Kummu, Joseph Guillaume, Hans Moel, Stephanie Eisner, Martina Flörke, Miina Porkka, Stefan Siebert, Ted I.E. Veldkamp, and Philip Ward. The world's road to water scarcity: Shortage and stress in the 20th century and pathways towards sustainability. *Scientific Reports*, 6:38495, 12 2016. doi: 10.1038/srep38495.

[6] Christopher Martin. Hygroscopic Cooling Tower for Reduced HVAC Water Consumption: DEMONSTRATION PLAN. 2018. URL `https://www.mcwd.org/gsa_water_supply.html`.

[7] CEC (California Energy Commission). NONRESIDENTIAL COMPLIANCE MANUAL FOR THE 2019 BUILDING ENERGY EFFICIENCY STANDARDS, 2019. URL `https://ww2.energy.ca.gov/2018publications/CEC-400-2018-018/Compliance_Manual-Complete_without_forms.pdf`.

[8] NOAA (National Centers for Environmental Information). Data Tools: 1981-2010 Normals, 2010. URL `https://www.ncdc.noaa.gov/cdo-web/datatools/normals`.

[9] NIDIS (National Integrated Drought Information System). Drought in California, 2020. URL https://www.drought.gov/drought/states/california.

[10] Landon Marston and Megan Konar. Drought impacts to water footprints and virtual water transfers of the Central Valley of California. *Water Resources Research*, 06 2017. doi: 10.1002/2016WR020251.

[11] Munish K. Chandel, Lincoln F. Pratson, and Robert B. Jackson. The potential impacts of climate-change policy on freshwater use in thermoelectric power generation. *Energy Policy*, 39(10):6234 – 6242, 2011. ISSN 0301-4215. doi: https://doi.org/10.1016/j.enpol.2011.07.022. URL http://www.sciencedirect.com/science/article/pii/S0301421511005465. Sustainability of biofuels.

[12] EPA (U.S. Environmental Protection Agency). Emission Factors for Greenhouse Gas Inventories, 2020. URL https://www.epa.gov/energy/emissions-generation-resource-integrated-database-egrid.

[13] EPA (U.S. Environmental Protection Agency). Cooling Water Intake Structures—CWA y316(b), Basic Information, 2020. URL http://water.epa.gov/lawsregs/lawsguidance/cwa/316b/basic.cfm#316bS.

[14] C. A. Dieter, M. A. Maupin, R. R. Caldwell, M. A. Harris, T. I. Ivahnenko, J. K. Lovelace, N. L. Barber, and K. S. Linsey. Estimated use of water in the United States in 2015. *U.S. Geological Survey*, 2018. doi: 10.3133/cir1441.

[15] EIA (U.S. Energy Information Administration). Form EIA-923 detailed data with previous form data (EIA-906/920), 2020. URL https://www.eia.gov/electricity/data/eia923/.

[16] Landon Marston, Yufei Ao, Megan Konar, Mesfin Mekonnen, and Arjen Hoekstra. High-Resolution Water Footprints of Production of the United States. *Water Resources Research*, 54, 02 2018. doi: 10.1002/2017WR021923.

[17] Angineh Zohrabian and Kelly Sanders. Assessing the impact of drought on the emissions- and water-intensity of California's transitioning power sector. *Energy Policy*, 123:461–470, 12 2018. doi: 10.1016/j.enpol.2018.09.014.

[18] Tim Diehl and Melissa Harris. Withdrawal and consumption of water by thermoelectric power plants in the United States, 2010. 01 2014. doi: 10.3133/sir20145184.

[19] Melissa Harris and Tim Diehl. Withdrawal and consumption of water by thermoelectric power plants in the United States, 2015. 0 2019. doi: 10.3133/sir20195103.

[20] Jordan Macknick, Robin Newmark, Garvin Heath, and K.C. Hallett. Operational Water Consumption and Withdrawal Factors for Electricity Generating Technologies: A Review of Existing Literature. *Environmental Research Letters*, 7, 10 2012. doi: 10.2172/1009674.

[21] Peter Gleick. Environmental consequences of hydroelectric development: The role of facility size and type. *Energy*, 17:735–747, 08 1992. doi: 10.1016/0360-5442(92)90116-H.

[22] P. Torcellini, N. Long, and R. Judkoff. Consumptive Water Use for U.S. Power Production. *NREL/TP-550-33905*, 12 2010. doi: 10.2172/15005918.

[23] Emily Grubert. Water Consumption from Hydroelectricity in the United States. *Advances in Water Resources*, 96, 07 2016. doi: 10.1016/j.advwatres.2016.07.004.

[24] EPA (U.S. Environmental Protection Agency). Emission Factors for Greenhouse Gas Inventories, 2018. URL `https://www.epa.gov/sites/production/files/2018-03/documents/emission-factors_mar_2018_0.pdf`.

[25] Christopher M. Chini and Ashlynn S. Stillwell. The State of U.S. Urban Water: Data and the Energy-Water Nexus. *Water Resources Research*, 54, 02 2018. doi: 10.1002/2017WR022265.

[26] R. Goldstein and W. Smith. Water and Sustainability: U.S. Electricity Consumption for Water Supply Treatment—The Next Half Century. 2000. doi: 1006787. URL `https://www.epri.com/research/products/000000000001006787`.

[27] Kelly T. Sanders and Michael Webber. Evaluating the energy consumed for water use in the united states. *Environmental Research Letters*, 114145224:70–34034, 09 2012. doi: 10.1088/1748-9326/7/3/034034.

[28] Christopher M. Chini and Ashlynn S. Stillwell. The Urban Energy-Water Nexus: Utility-Level Water Flows and Embedded Energy, 2018. URL `https://doi.org/10.4211/hs.df04c29d0ff64de0ace2d29145dd7680`.

[29] MCWD (Marina Coast Water District). Securing Our Water Supply, 2020. URL `https://www.mcwd.org/gsa_water_supply.html`.

[30] LAO (Legislative Analyst's Office). Assessing California's Climate Policies—Electricity Generation, 2020. URL `https://lao.ca.gov/Publications/Report/4131#Overview_of_Electricity_Sector_Emissions`.

[31] OEHHA (California Office of Environmental Health Hazard Assessment). OEHHA, 2020. URL `https://oehha.ca.gov/epic/impacts-physical-systems/snowmelt-runoff`.

[32] EPA (U.S. Environmental Protection Agency). National Pollutant Discharge Elimination System-Final Regulations To Establish Requirements for Cooling Water Intake Structures at Existing Facilities and Amend Requirements at Phase I Facilities., 2014. URL `https://www.govinfo.gov/content/pkg/FR-2014-08-15/pdf/2014-12164.pdf`.

[33] NRDC (Natural Resources Defense Council). Power Plant Cooling Water and Clean Water Act Section 316(b): The Need to Modernize U.S. Power Plants and Protect our Water Resources, 2020. URL https://www.nrdc.org/sites/default/files/powerplantcooling.pdf.

[34] N. Madden, A. Lewis, and M. Davis. Thermal effluent from the power sector: An analysis of once-through cooling system impacts on surface water temperature. *Environmental Research Letters*, 8:035006, 07 2013. doi: 10.1088/1748-9326/8/3/035006.

[35] Erich Hester and Martin Doyle. Human Impacts to River Temperature and Their Effects on Biological Processes: A Quantitative Synthesis 1. *JAWRA Journal of the American Water Resources Association*, 47:571 – 587, 03 2011. doi: 10.1111/j.1752-1688.2011.00525.x.

[36] EIA (U.S. Energy Information Administration). Form EIA-923 Power Plant Operations Report Instructions, 2020. URL https://www.eia.gov/survey/form/eia_923/instructions.pdf.

[37] EIA (U.S. Energy Information Administration). Form EIA-860 detailed data with previous form data (EIA-860A/860B), 2019. URL https://www.eia.gov/electricity/data/eia860/.

[38] EIA (U.S. Energy Information Administration). Form EIA-860 Instructions Annual Electric Generator Report, 2019. URL https://www.eia.gov/survey/form/eia_860/instructions.pdf.

[39] California State Water Resources Control Board. Statewide water quality control policy on the use of coastal and estuarine waters for power plant cooling, 2010. URL https://www.waterboards.ca.gov/water_issues/programs/ocean/cwa316/docs/cwa316may2010/otcpolicy_final050410.pdf.

[40] Brian Richter, Dominique Bartak, Peter Caldwell, Kyle Davis, Peter Debaere, Arjen Hoekstra, Tianshu Li, Landon Marston, Ryan McManamay, Mesfin Mekonnen, Benjamin Ruddell, Richard Rushforth, and Tara Troy. Water scarcity and fish imperilment driven by beef production. *Nature Sustainability*, 3:319–328, 04 2020. doi: 10.1038/s41893-020-0483-z.

[41] Ertug Ercin and Arjen Hoekstra. Water footprint scenarios for 2050: A global analysis. *Environment international*, 64C:71–82, 12 2013. doi: 10.1016/j.envint.2013.11.019.

[42] Eugenia Kalnay and Ming Cai. Impact of Urbanization and Land-Use Change on Climate. *Nature*, 423:528–31, 06 2003. doi: 10.1038/nature01675.

[43] Brooke Anderson and Michelle Bell. Heat Waves in the United States: Mortality Risk during Heat Waves and Effect Modification by Heat Wave Characteristics in 43 USA Communities. *Environmental health perspectives*, 119:210–8, 11 2010. doi: 10.1289/ehp.1002313.

[44] T. Chakraborty, Angel Hsu, Diego Manya, and Glenn Sheriff. Disproportionately higher exposure to urban heat in lower-income neighborhoods: a multi-city perspective. *Environmental Research Letters*, 14, 08 2019. doi: 10.1088/1748-9326/ab3b99.

[45] Paul Barlow and Eric Reichard. Saltwater intrusion in coastal regions of North America. *Hydrogeology Journal*, 18:247–260, 02 2010. doi: 10.1007/s10040-009-0514-3.

[46] Caroline Scruggs, Claudia Pratesi, and John Fleck. Direct potable water reuse in five arid inland communities: an analysis of factors influencing public acceptance. *Journal of Environmental Planning and Management*, 63:1–30, 10 2019. doi: 10.1080/09640568.2019.1671815.

[47] Nazar Kholod, Meredydd Evans, Raymond Pilcher, Volha Roshchanka, Felicia Ruiz, Michael Coté, and Ron Collings. Global methane emissions from coal mining to continue growing even with declining coal production. *Journal of Cleaner Production*, 256, 11 2020. doi: 10.1016/j.jclepro.2020.120489.

[48] R. Howarth, Renee Santoro, and Anthony Ingraffea. Methane and the Greenhouse-Gas Footprint of Natural Gas from Shale Formations. *Climatic Change*, 106:679–690, 06 2011. doi: 10.1007/s10584-011-0061-5.

[49] EIA (U.S. Energy Information Administration). Hydraulically fractured wells provide two-thirds of U.S. natural gas production, 2016. URL `https://www.eia.gov/todayinenergy/detail.php?id=26112`.

[50] EPA (U.S. Environmental Protection Agency). Basic Information of Air Emissions Factors and Quantification, 2019. URL `https://www.epa.gov/air-emissions-factors-and-quantification/basic-information-air-emissions-factors-and-quantification`.

APPENDIX A

GREENHOUSE GAS EMISSIONS FIGURES

A.1 Monterey Bay 2019: Normalized Without and With Heat Exchanger

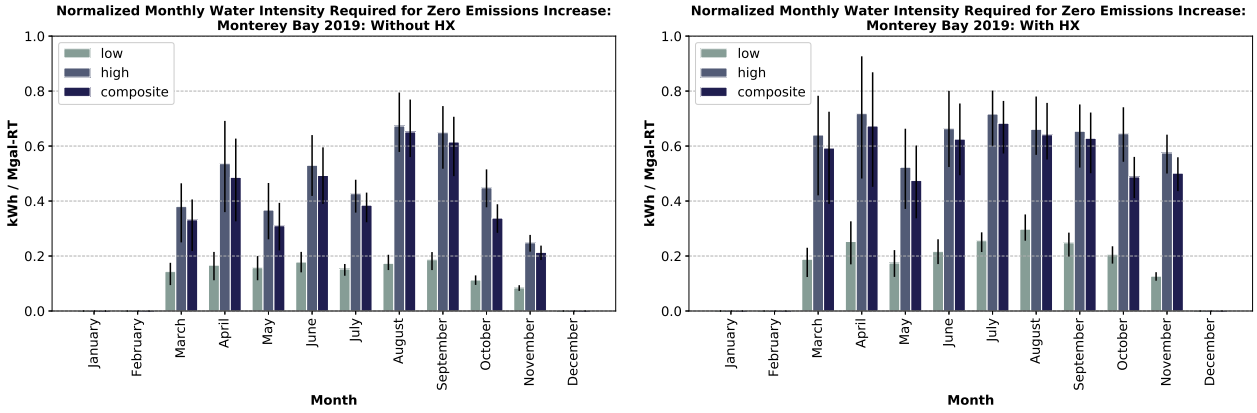

(a) Without Heat Exchanger

(b) With Heat Exchanger

Figure A.1: The weighted average of monthly water and wastewater treatment energy intensity (in kWh per million gallon) required to achieve zero GHG emissions (in $CO_{2,eqv}$) increase associated with the switch to the hygroscopic cooling system at the DoD Center Monterey Bay (DCMB) cooling tower in 2019 were normalized by refrigeration ton (RT) of the cooling tower capacity. The energy intensity of water is the weighted average of the energy required for sourcing, treating, and conveying water and the energy require for the conveyance and treatment of wastewater.

A.2 Fort Irwin 2019: Normalized Without and With Heat Exchanger

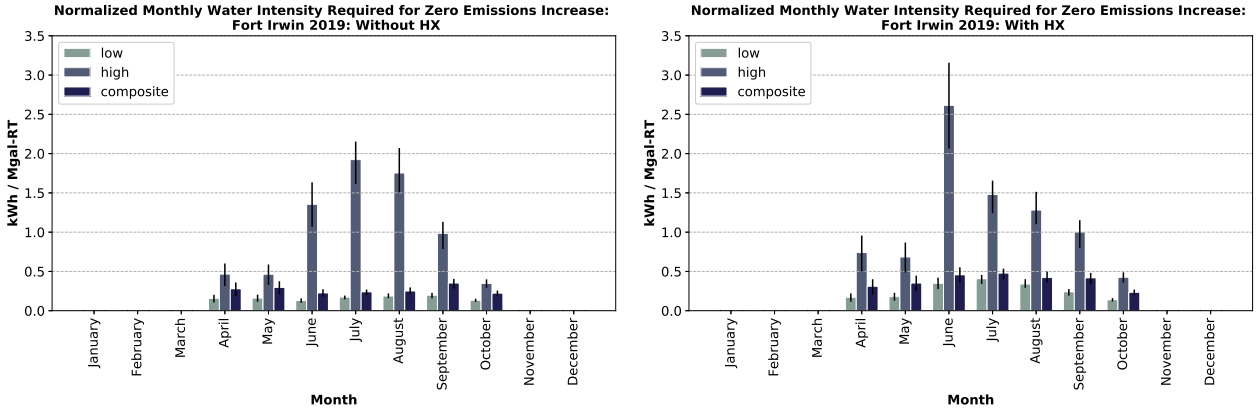

(a) Without Heat Exchanger

(b) With Heat Exchanger

Figure A.2: The weighted average of monthly water and wastewater treatment energy intensity (in kWh per million gallon) required to achieve zero GHG emissions (in $CO_{2,eqv}$) increase associated with the switch to the hygroscopic cooling system at the Fort Irwin cooling tower in 2019 were normalized by refrigeration ton (RT) of the cooling tower capacity. The energy intensity of water is the weighted average of the energy required for sourcing, treating, and conveying water and the energy require for the conveyance and treatment of wastewater.

A.3 Monterey Bay 2019: Non-Normalized Without and With Heat Exchanger

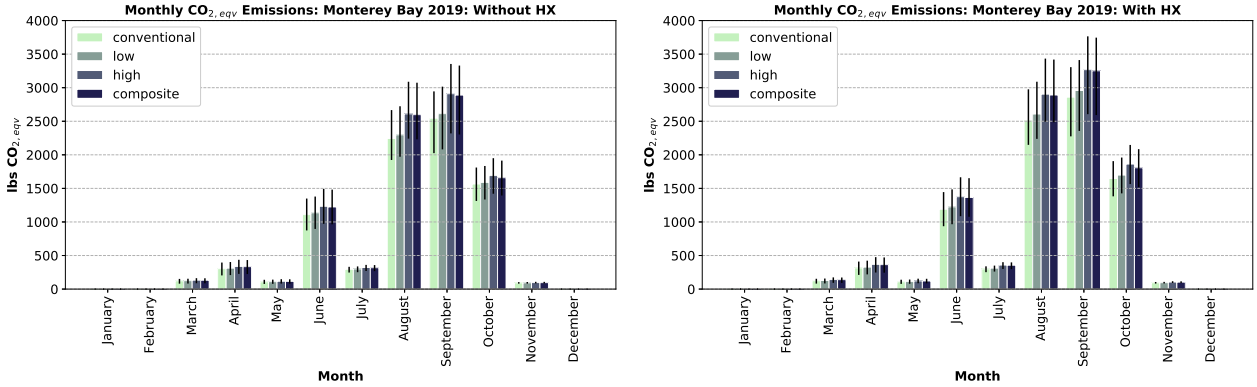

(a) Without Heat Exchanger (b) With Heat Exchanger

Figure A.3: The total monthly emissions (in $CO_{2,eqv}$) for the DoD Center Monterey Bay (DCMB) cooling tower in 2019.

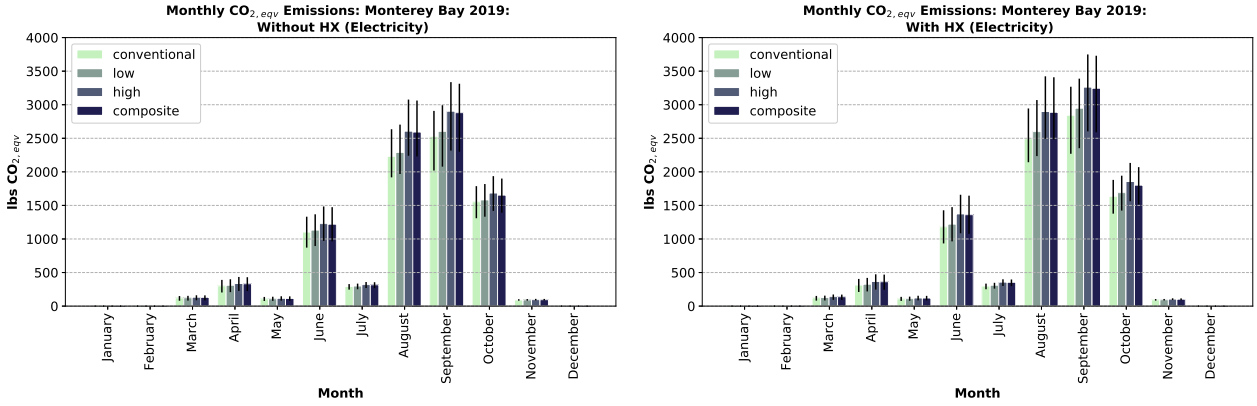

(a) Without Heat Exchanger (b) With Heat Exchanger

Figure A.4: The monthly emissions (in $CO_{2,eqv}$) associated with direct electricity usage for the DoD Center Monterey Bay (DCMB) cooling tower in 2019.

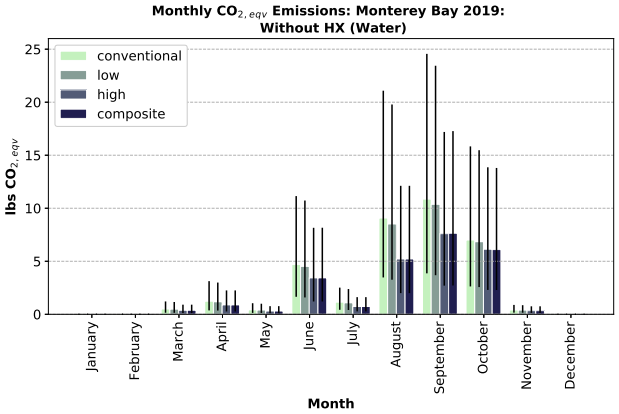

(a) Without Heat Exchanger

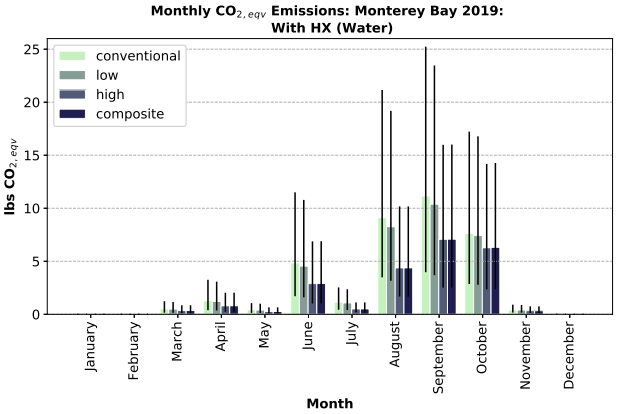

(b) With Heat Exchanger

Figure A.5: The monthly emissions (in $CO_{2,eqv}$) associated with direct water consumption by the DoD Center Monterey Bay (DCMB) cooling tower in 2019.

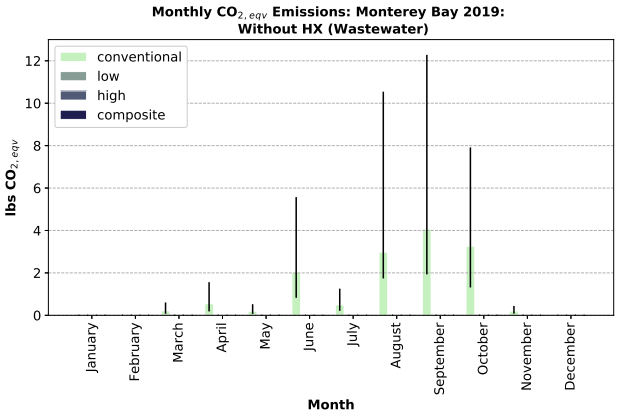

(a) Without Heat Exchanger

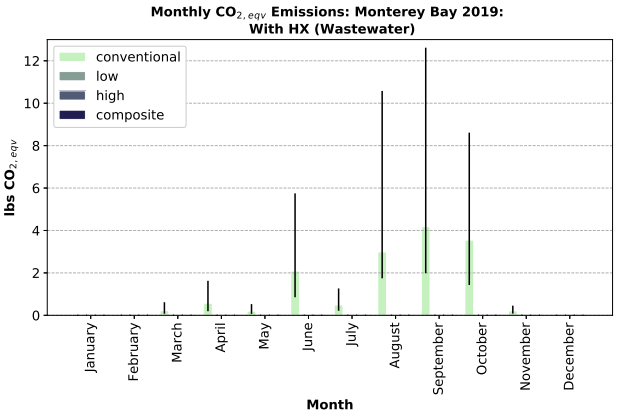

(b) With Heat Exchanger

Figure A.6: The monthly emissions (in $CO_{2,eqv}$) associated with wastewater discharged by the DoD Center Monterey Bay (DCMB) cooling tower in 2019.

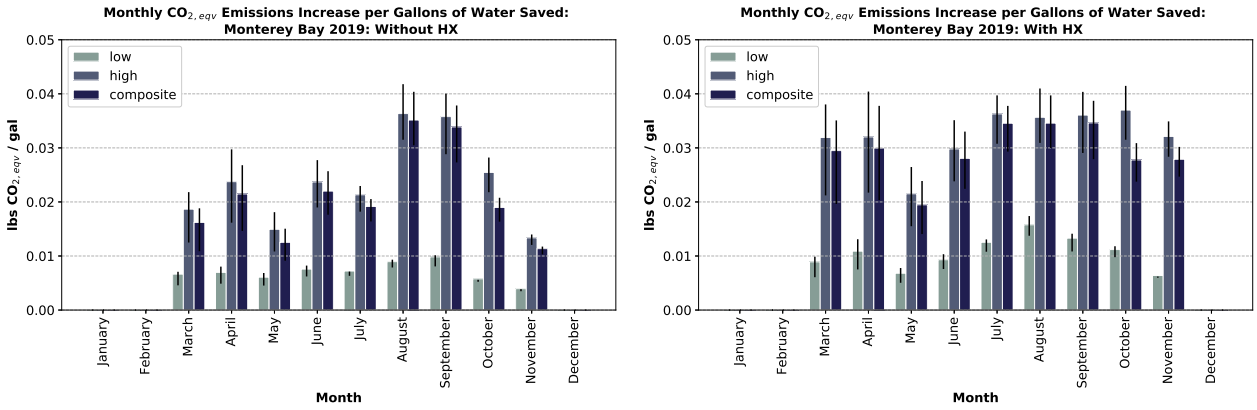

(a) Without Heat Exchanger (b) With Heat Exchanger

Figure A.7: The total monthly emissions (in $CO_{2,eqv}$) increase per gallon of water saved by the hygroscopic cooling system at the DoD Center Monterey Bay (DCMB) cooling tower in 2019.

A.4 Fort Irwin 2019: Non-Normalized Without and With Heat Exchanger

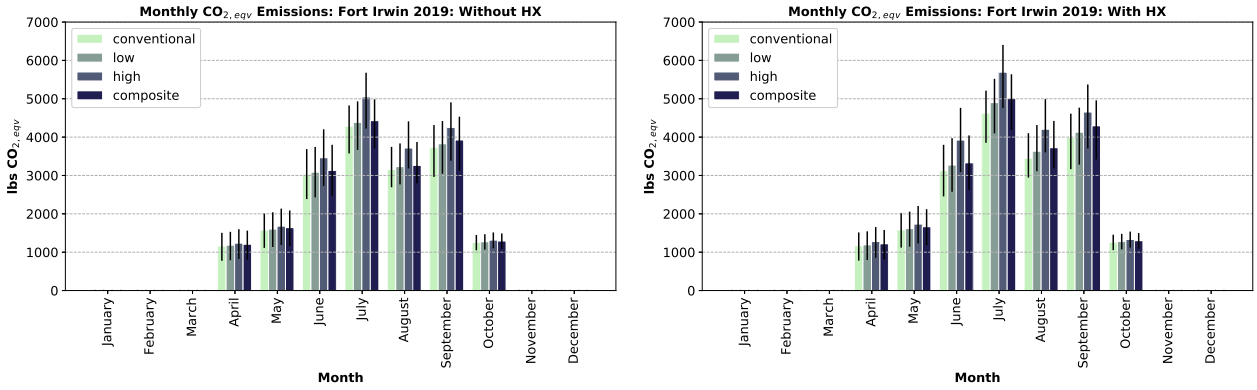

(a) Without Heat Exchanger (b) With Heat Exchanger

Figure A.8: The total monthly emissions (in $CO_{2,eqv}$)for the Fort Irwin cooling tower in 2019.

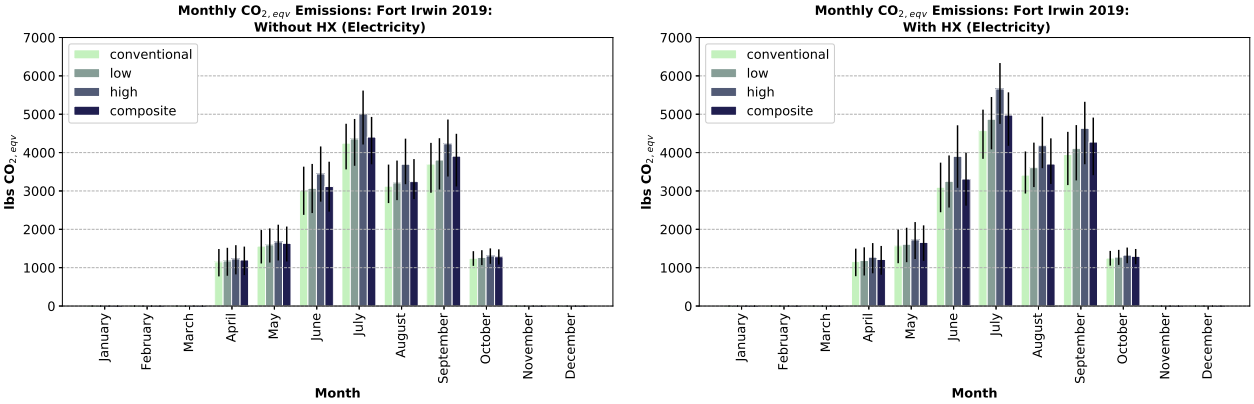

(a) Without Heat Exchanger

(b) With Heat Exchanger

Figure A.9: The monthly emissions (in $CO_{2,eqv}$) associated with direct electricity usage for the Fort Irwin cooling tower in 2019.

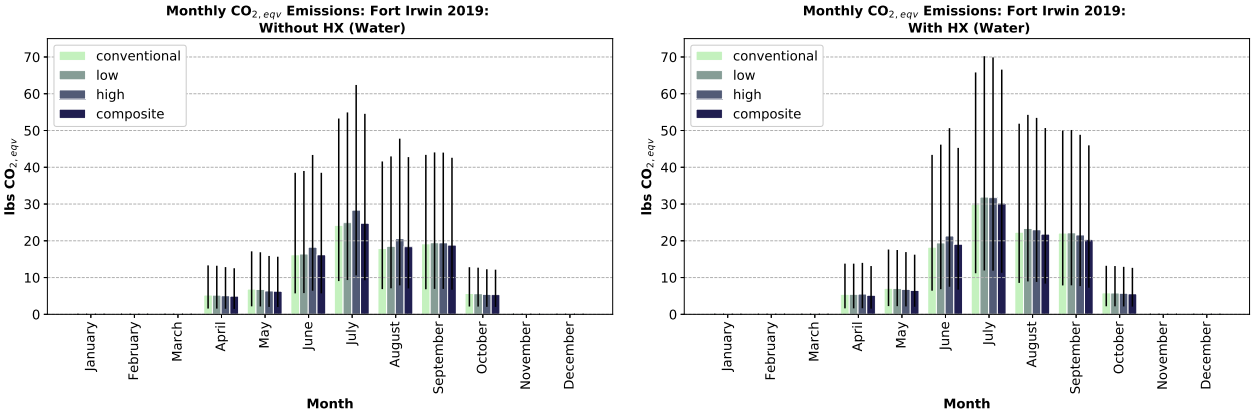

(a) Without Heat Exchanger

(b) With Heat Exchanger

Figure A.10: The monthly emissions (in $CO_{2,eqv}$) associated with direct water consumption by the Fort Irwin cooling tower in 2019.

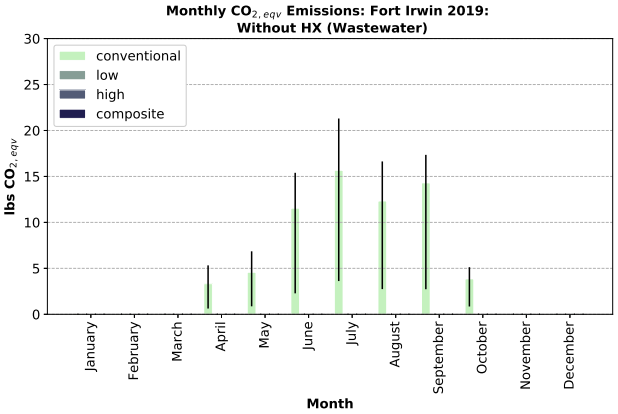

(a) Without Heat Exchanger

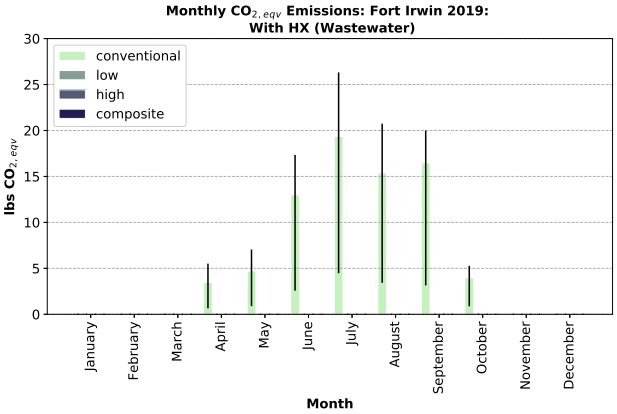

(b) With Heat Exchanger

Figure A.11: The monthly emissions (in $CO_{2,eqv}$) associated with wastewater discharged by the Fort Irwin cooling tower in 2019.

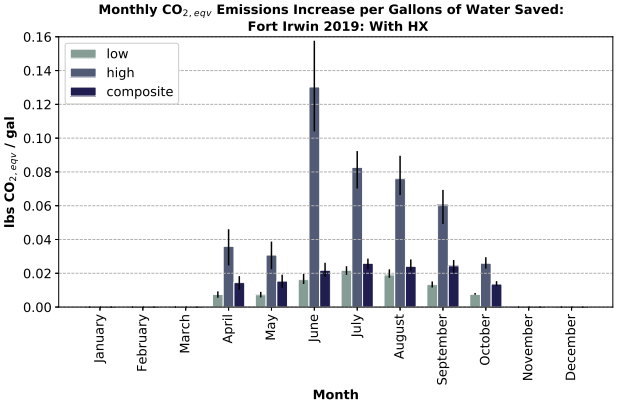

(a) Without Heat Exchanger

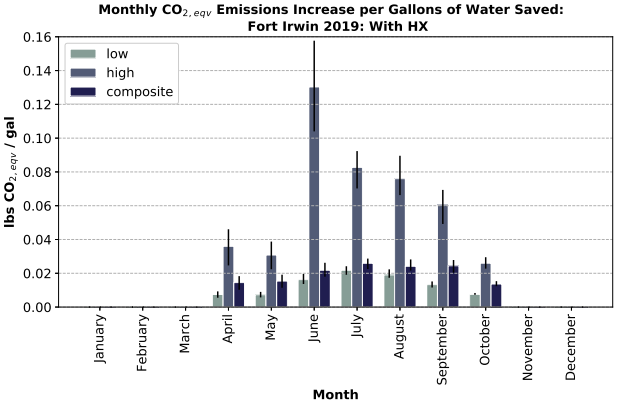

(b) With Heat Exchanger

Figure A.12: The total monthly emissions (in $CO_{2,eqv}$) increase per gallon of water saved by the hygroscopic cooling system at the Fort Irwin cooling tower in 2019.

A.5 Fort Irwin Normalized Without and With Heat Exchanger 2018

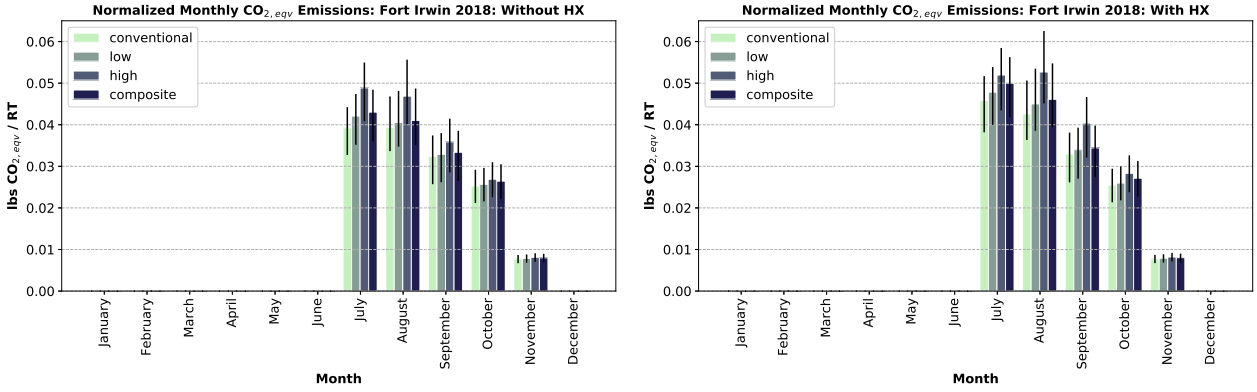

(a) Without Heat Exchanger (b) With Heat Exchanger

Figure A.13: The total monthly emissions (in $CO_{2,eqv}$)for the Fort Irwin cooling tower in 2018 were normalized by refrigeration ton (RT) of the cooling tower capacity.

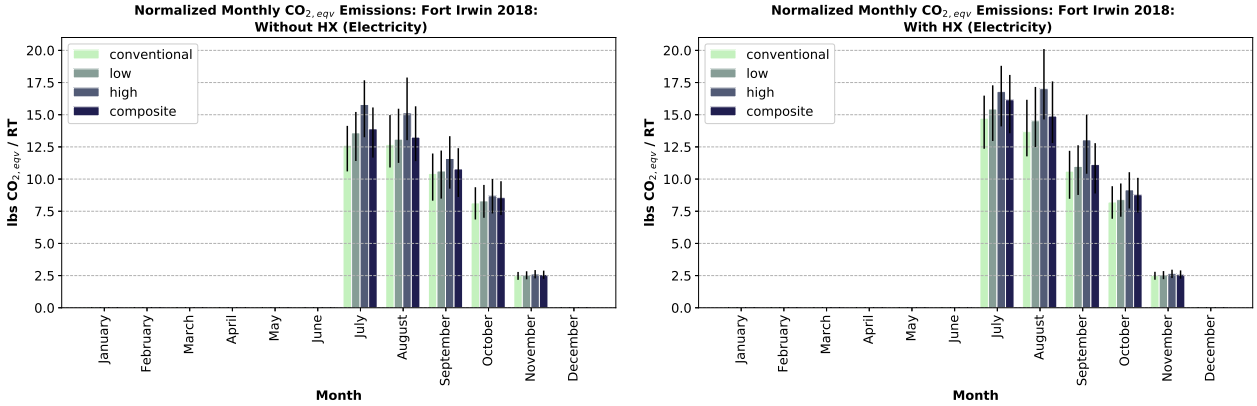

(a) Without Heat Exchanger (b) With Heat Exchanger

Figure A.14: The monthly emissions (in $CO_{2,eqv}$) associated with direct electricity usage for the Fort Irwin cooling tower in 2018 were normalized by refrigeration ton (RT) of the cooling tower capacity.

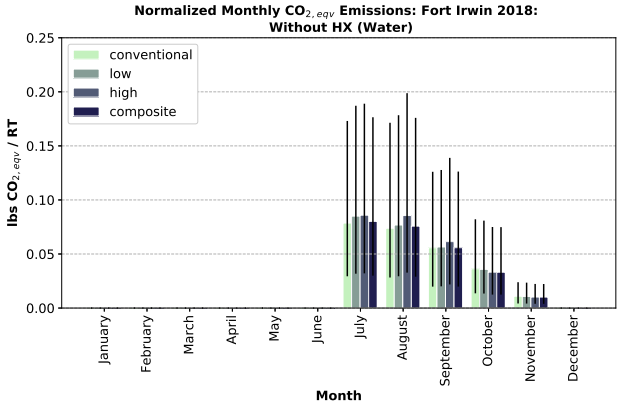

(a) Without Heat Exchanger

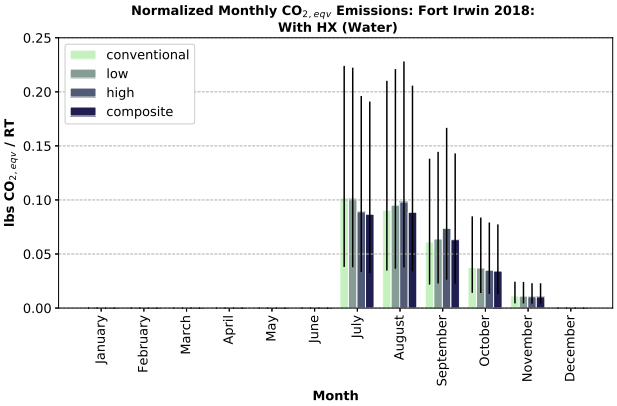

(b) With Heat Exchanger

Figure A.15: The monthly emissions (in $CO_{2,eqv}$) associated with direct water consumption by the Fort Irwin cooling tower in 2018 were normalized by refrigeration ton (RT) of the cooling tower capacity.

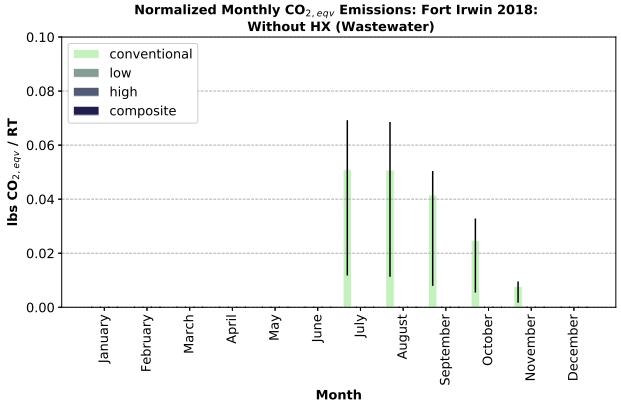

(a) Without Heat Exchanger

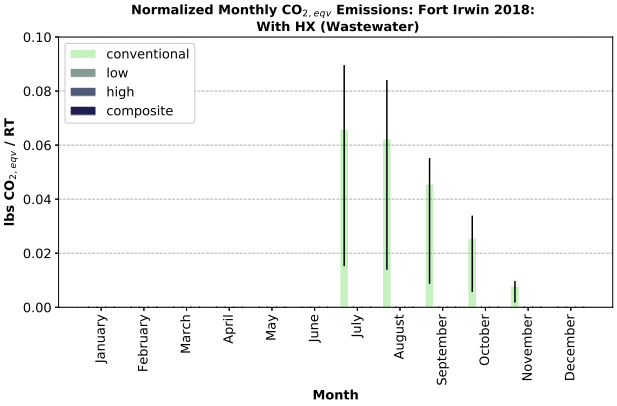

(b) With Heat Exchanger

Figure A.16: The monthly emissions (in $CO_{2,eqv}$) associated with wastewater discharged by the Fort Irwin cooling tower in 2018 were normalized by refrigeration ton (RT) of the cooling tower capacity.

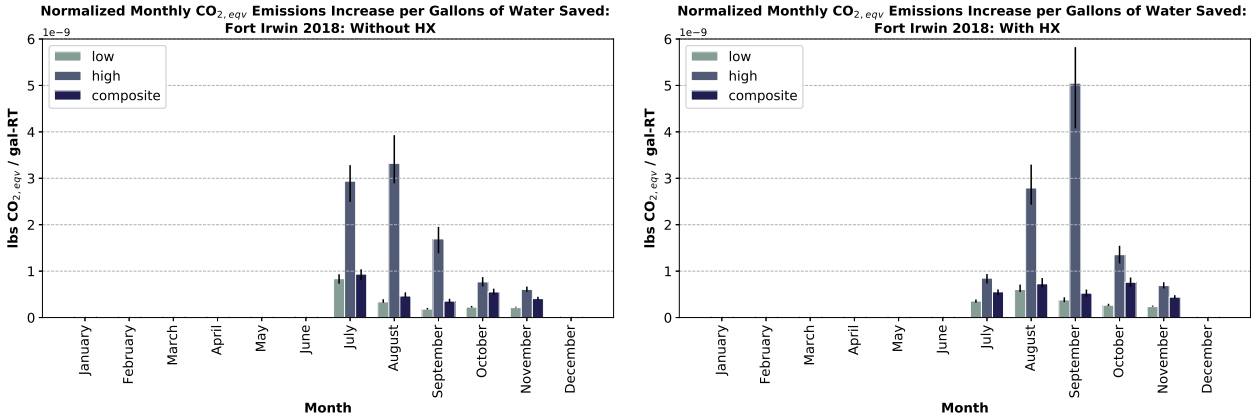

(a) Without Heat Exchanger (b) With Heat Exchanger

Figure A.17: The total monthly emissions (in $CO_{2,eqv}$) increase per gallon of water saved by the hygroscopic cooling system at the Fort Irwin cooling tower in 2018 were normalized by refrigeration ton (RT) of the cooling tower capacity.

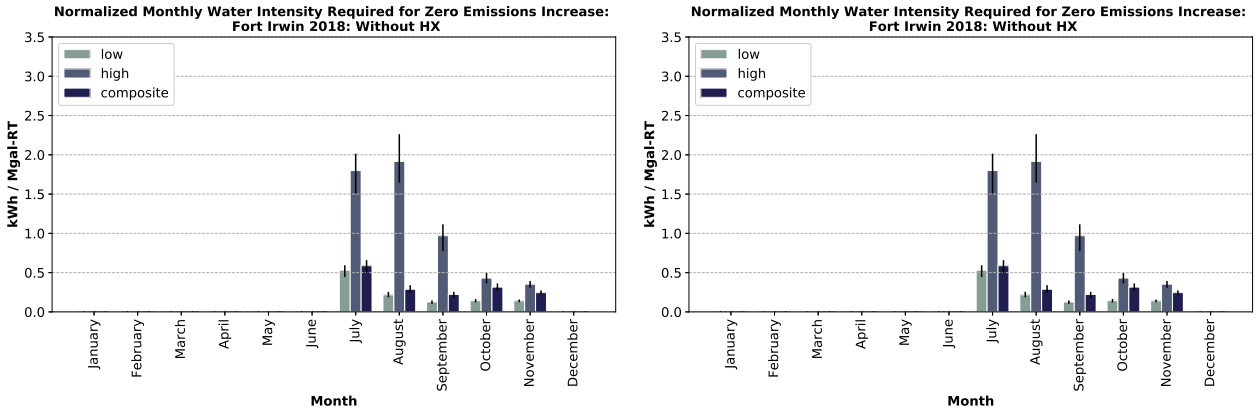

(a) Without Heat Exchanger (b) With Heat Exchanger

Figure A.18: The weighted average of monthly water and wastewater treatment energy intensity (in kWh per million gallon) required to achieve zero GHG emissions (in $CO_{2,eqv}$) increase associated with the switch to the hygroscopic cooling system at the Fort Irwin cooling tower in 2018 were normalized by refrigeration ton (RT) of the cooling tower capacity. The energy intensity of water is the weighted average of the energy required for sourcing, treating, and conveying water and the energy require for the conveyance and treatment of wastewater.

A.6 Fort Irwin Non-Normalized Without and With Heat Exchanger 2018

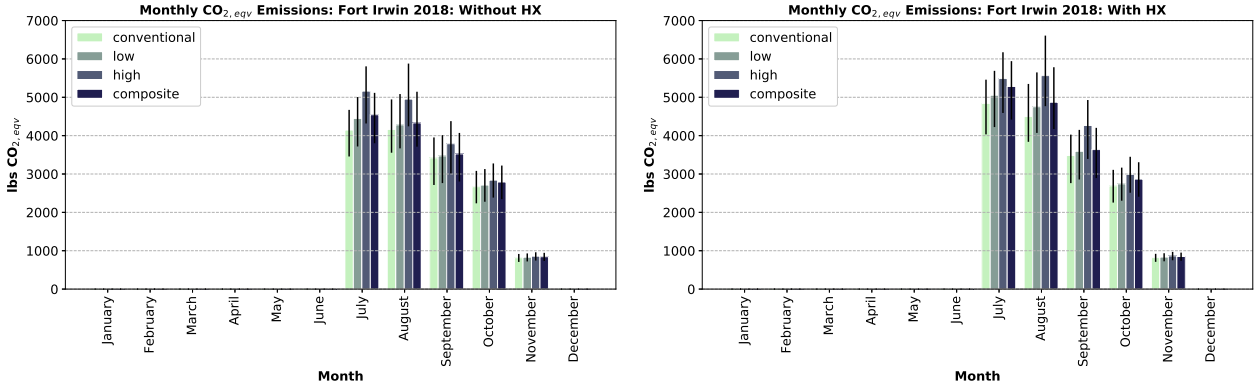

(a) Without Heat Exchanger (b) With Heat Exchanger

Figure A.19: The total monthly emissions (in $CO_{2,eqv}$)for the Fort Irwin cooling tower in 2018.

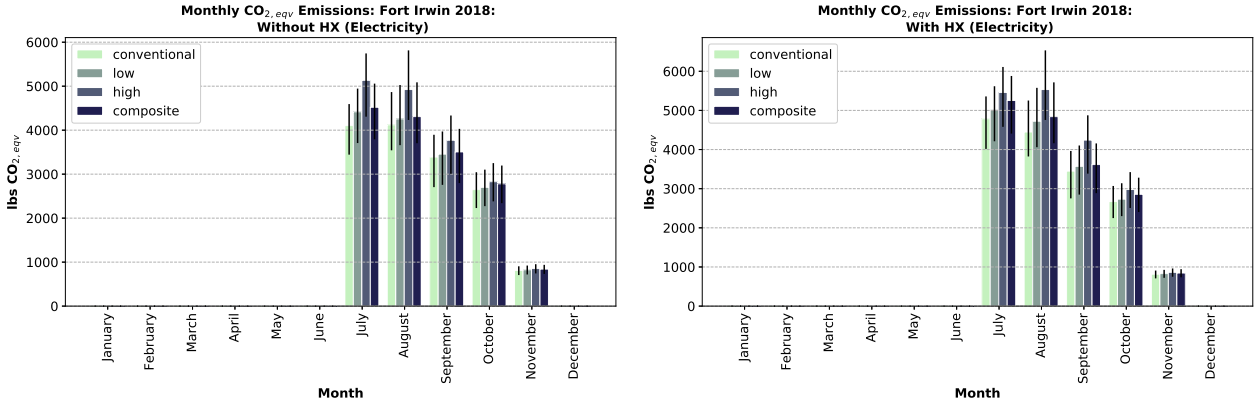

(a) Without Heat Exchanger (b) With Heat Exchanger

Figure A.20: The monthly emissions (in $CO_{2,eqv}$) associated with direct electricity usage for the Fort Irwin cooling tower in 2018.

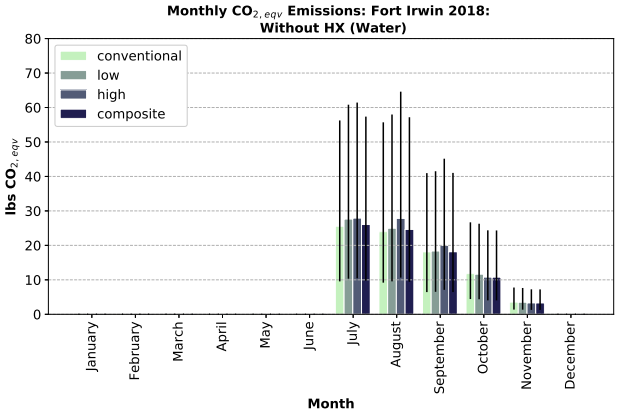

(a) Without Heat Exchanger

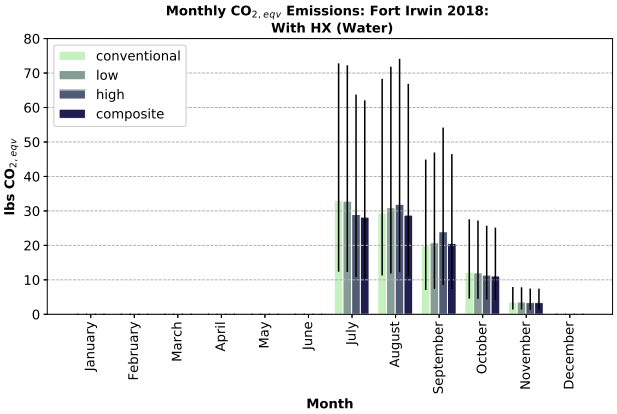

(b) With Heat Exchanger

Figure A.21: The monthly emissions (in $CO_{2,eqv}$) associated with direct water consumption by the Fort Irwin cooling tower in 2018.

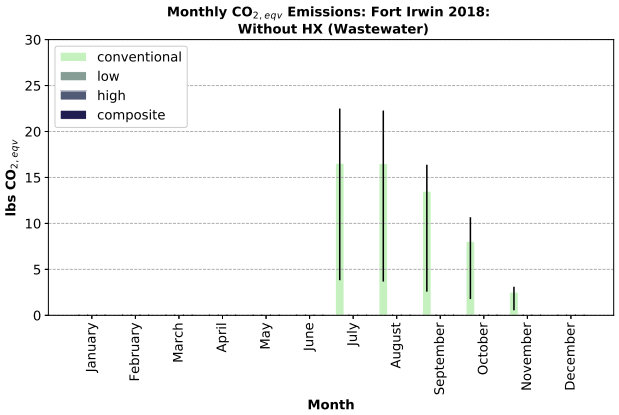

(a) Without Heat Exchanger

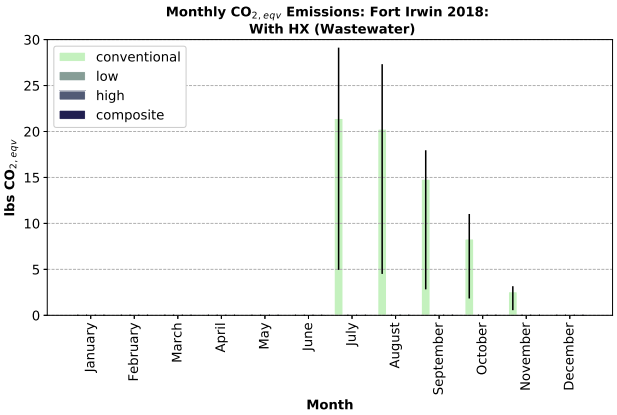

(b) With Heat Exchanger

Figure A.22: The monthly emissions (in $CO_{2,eqv}$) associated with wastewater discharged by the Fort Irwin cooling tower in 2018.

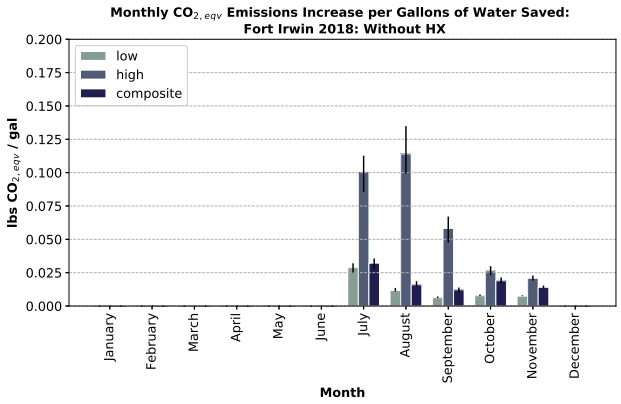

(a) Without Heat Exchanger

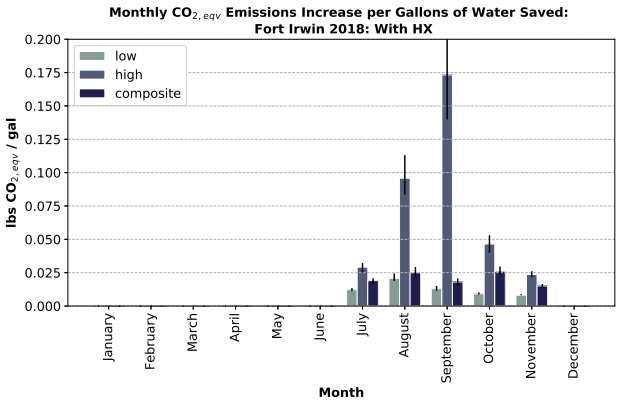

(b) With Heat Exchanger

Figure A.23: The total monthly emissions (in $CO_{2,eqv}$) increase per gallon of water saved by the hygroscopic cooling system at the Fort Irwin cooling tower in 2018.

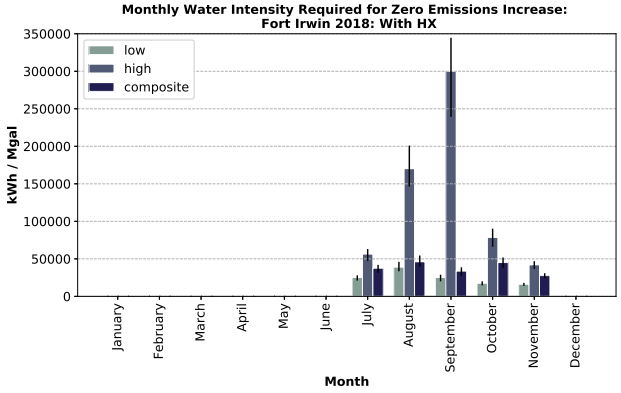

(a) Without Heat Exchanger

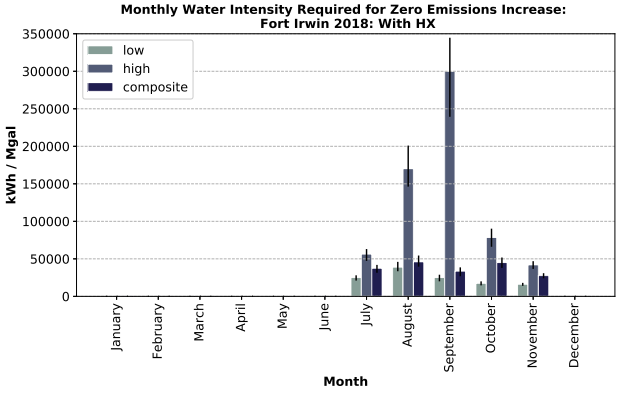

(b) With Heat Exchanger

Figure A.24: The weighted average of monthly water and wastewater treatment energy intensity (in kWh per million gallon) required to achieve GHG emissions (in $CO_{2,eqv}$) increase associated with the switch to the hygroscopic cooling system for the Fort Irwin cooling tower in 2018. The energy intensity of water is the weighted average of the energy required for sourcing, treating, and conveying water and the energy require for the conveyance and treatment of wastewater.

APPENDIX B

WATER WITHDRAWAL AND CONSUMPTION FIGURES

B.1 Monterey Bay 2019: Non-Normalized Without and With Heat Exchanger

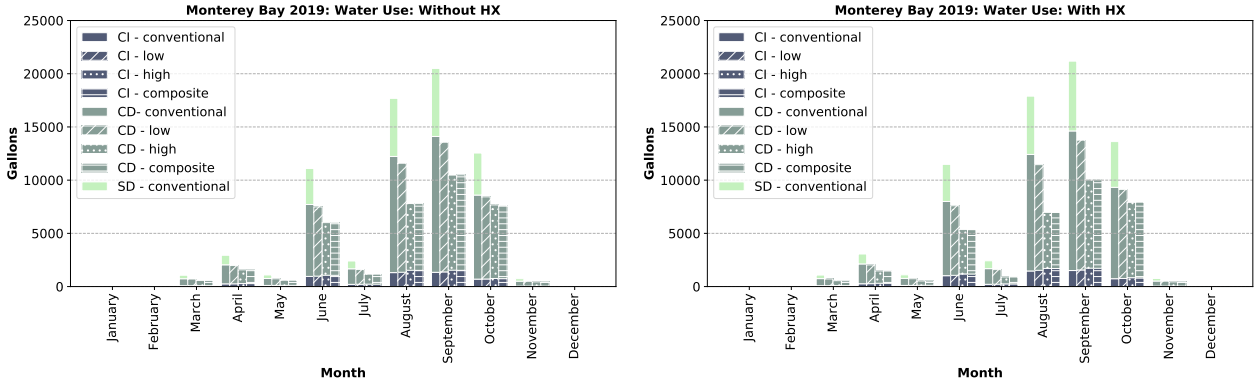

(a) Without Heat Exchanger

(b) With Heat Exchanger

Figure B.1: The monthly direct and indirect water usage by the DoD Center Monterey Bay (DCMB) cooling tower in 2019. Total direct and indirect water usage is is the sum of indirect consumption associated with electricity use (CI), direct consumption (CD), and direct wastewater discharged to the sewer (SD).

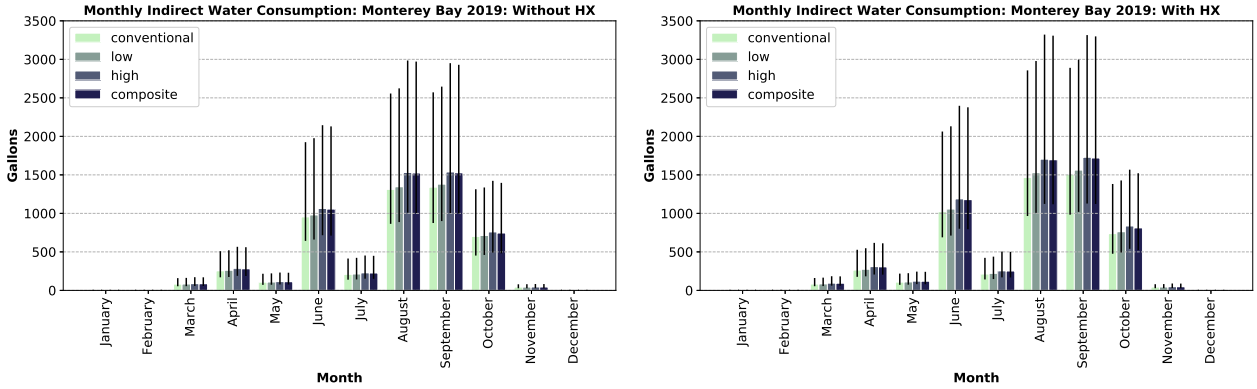

(a) Without Heat Exchanger (b) With Heat Exchanger

Figure B.2: The monthly indirect water consumption by the DoD Center Monterey Bay (DCMB) cooling tower in 2019.

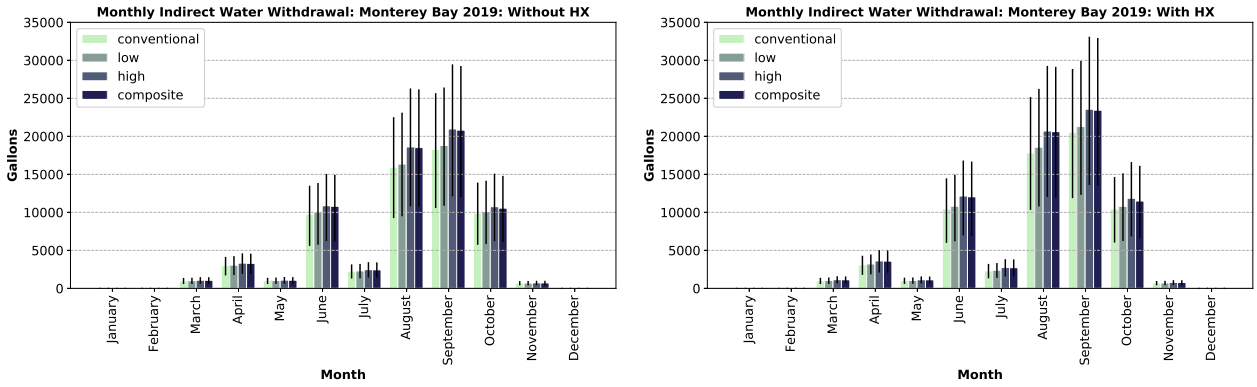

(a) Without Heat Exchanger (b) With Heat Exchanger

Figure B.3: The monthly indirect water withdrawal by the DoD Center Monterey Bay (DCMB) cooling tower in 2019.

B.2 Fort Irwin 2019: Non-Normalized Without and With Heat Exchanger

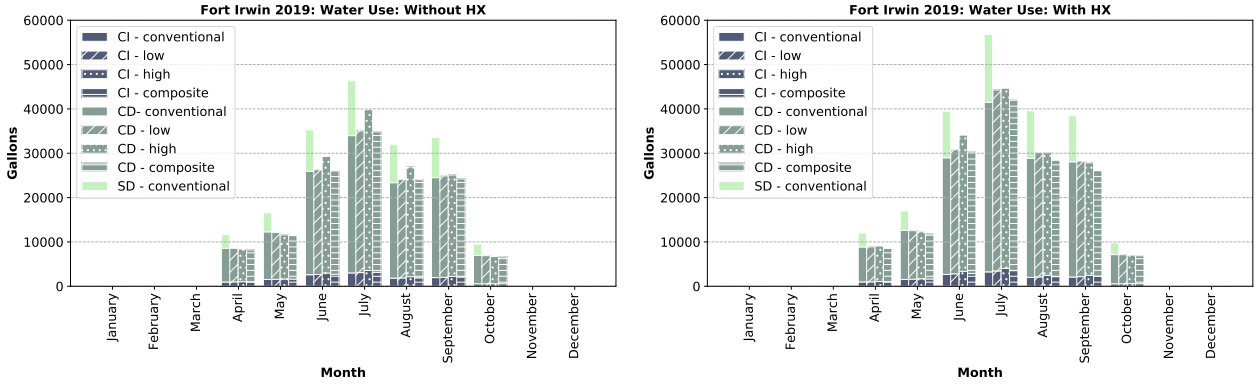

(a) Without Heat Exchanger (b) With Heat Exchanger

Figure B.4: The monthly direct and indirect water usage by the Fort Irwin cooling tower in 2019. Total direct and indirect water usage is is the sum of indirect consumption associated with electricity use, direct consumption (CD), and direct wastewater discharged to the sewer (SD).

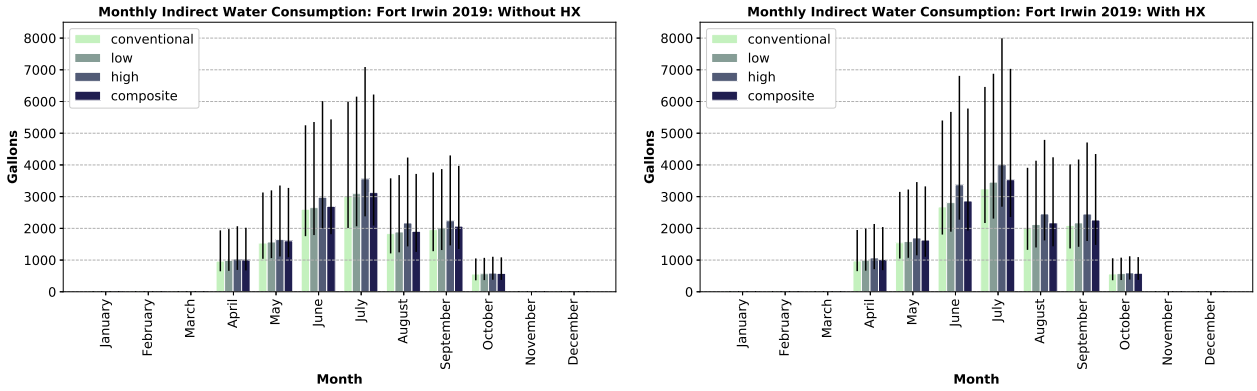

(a) Without Heat Exchanger (b) With Heat Exchanger

Figure B.5: The monthly indirect water consumption by the Fort Irwin cooling tower in 2019.

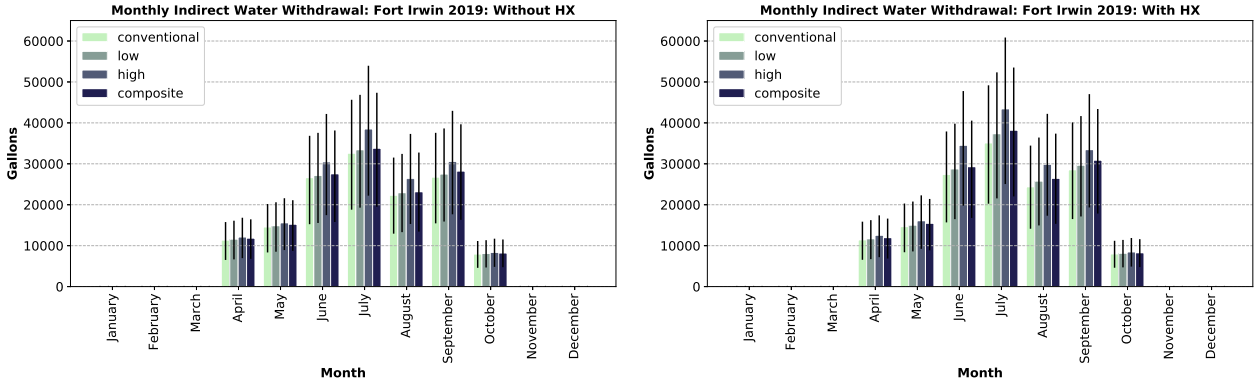

(a) Without Heat Exchanger (b) With Heat Exchanger

Figure B.6: The monthly indirect water withdrawal by the Fort Irwin cooling tower in 2019.

B.3 Fort Irwin 2018: Non-Normalized Without and With Heat Exchanger

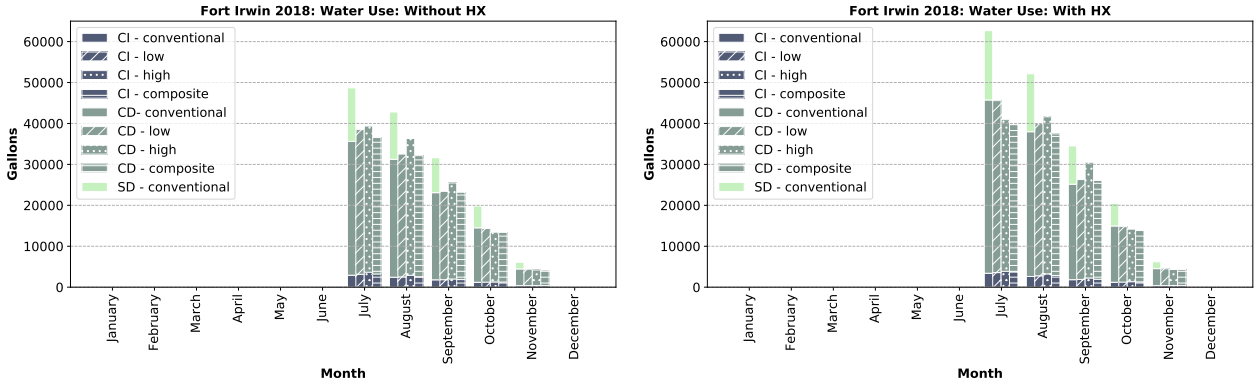

(a) Without Heat Exchanger (b) With Heat Exchanger

Figure B.7: The monthly direct and indirect water usage by the Fort Irwin cooling tower in 2018. Total direct and indirect water usage is is the sum of indirect consumption associated with electricity use, direct consumption (CD), and direct wastewater discharged to the sewer (SD).

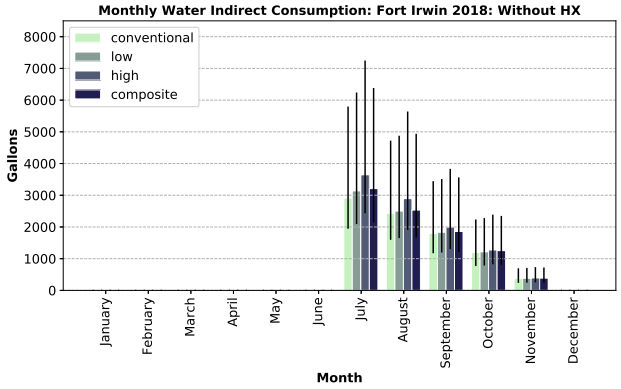

(a) Without Heat Exchanger

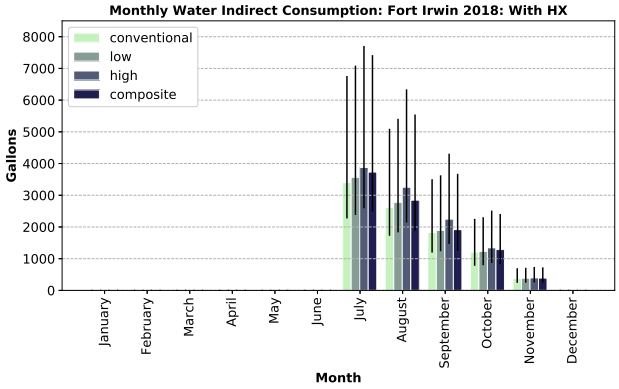

(b) With Heat Exchanger

Figure B.8: The monthly indirect water consumption by the Fort Irwin cooling tower in 2018.

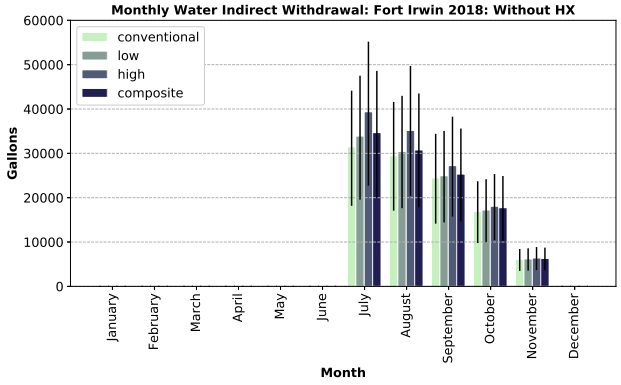

(a) Without Heat Exchanger

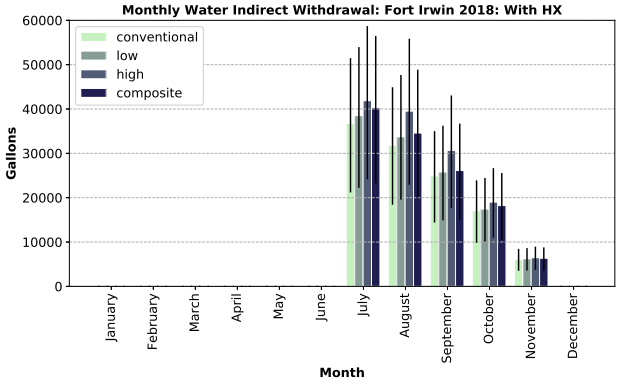

(b) With Heat Exchanger

Figure B.9: The monthly indirect water withdrawal by the Fort Irwin cooling tower in 2018.

B.4 Fort Irwin 2018: Normalized Without and With Heat Exchanger

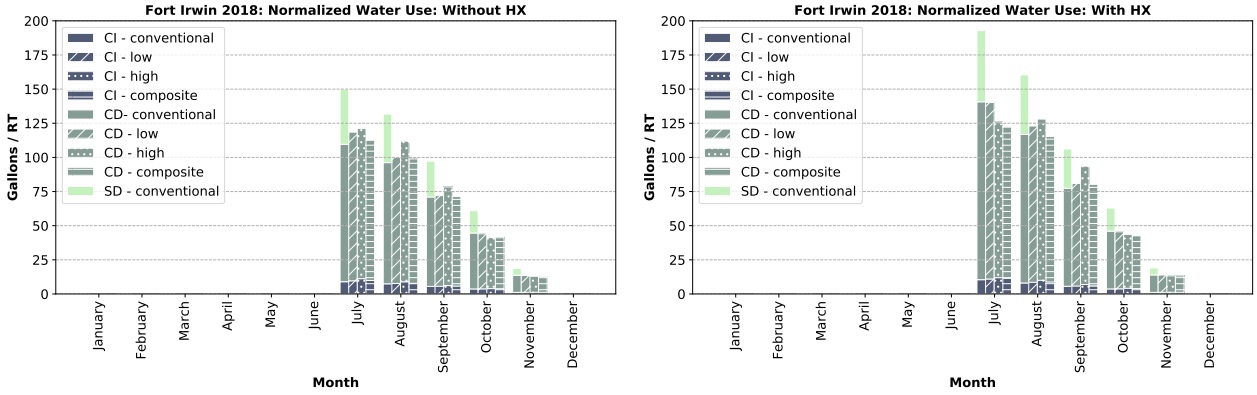

(a) Without Heat Exchanger (b) With Heat Exchanger

Figure B.10: The monthly direct and indirect water usage by the Fort Irwin cooling tower in 2018 was normalized by refrigeration ton (RT) of the cooling tower capacity. Total direct and indirect water usage is is the sum of indirect consumption associated with electricity use, direct consumption (CD), and direct wastewater discharged to the sewer (SD).

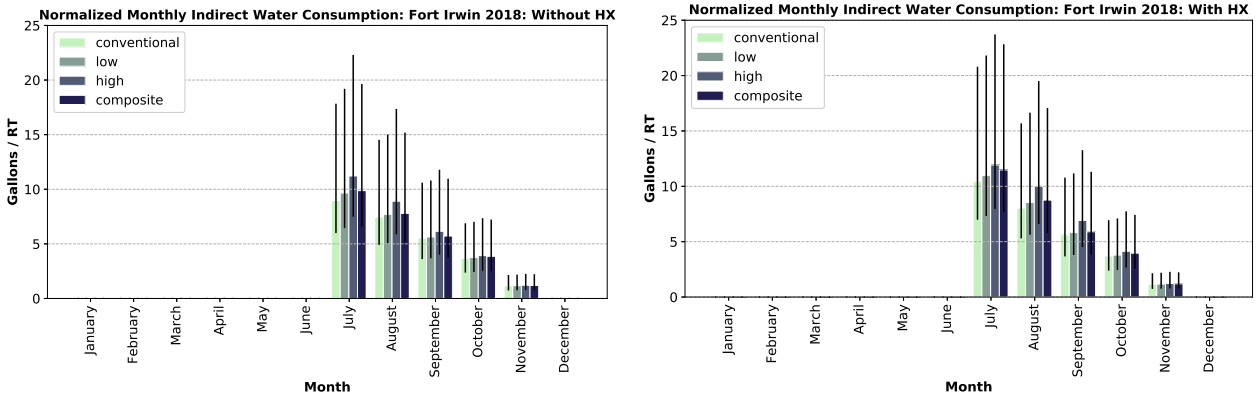

(a) Without Heat Exchanger (b) With Heat Exchanger

Figure B.11: The monthly indirect water consumption by the Fort Irwin cooling tower in 2018 was normalized by refrigeration ton (RT) of the cooling tower capacity.

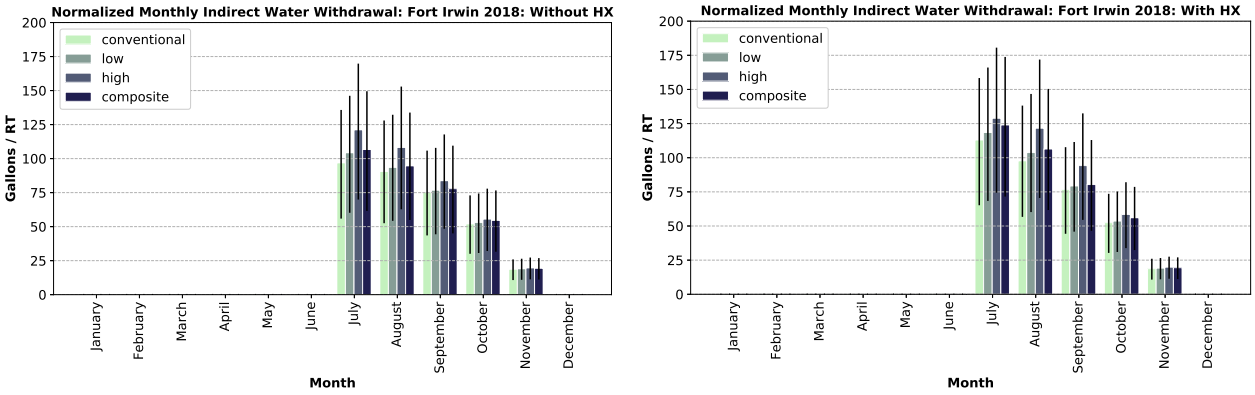

(a) Without Heat Exchanger

(b) With Heat Exchanger

Figure B.12: The monthly indirect water withdrawal by the Fort Irwin cooling tower in 2018 was normalized by refrigeration ton (RT) of the cooling tower capacity.